[28] Y. Kawano, Y. Tanaka, N. Misawa, R. Tanaka, J.I. Kira, T. Kimura, M. Fukushi, K. Sano, T. Goto, M. Nakai, T. Kobayashi, N. Yamamoto, Y. Koyanagi, Mutational analysis of human immunodeficiency virus type 1 (HIV-1) accessory genes: requirement of a site in the nef gene for HIV-1 replication in activated $CD4^+$ T cells in vitro and in vivo, J. Virol. 71 (1997) 8456–8466.

[29] J.A. Zack, S.J. Arrigo, S.R. Weitsman, A.S. Go, A. Haislip, I.S. Chen, HIV-1 entry into quiescent primary lymphocytes: molecular analysis reveals a labile, latent viral structure, Cell 61 (1990) 213–222.

[30] S.J. Neil, T. Zang, P.D. Bieniasz, Tetherin inhibits retrovirus release and is antagonized by HIV-1 Vpu, Nature 451 (2008) 425–430.

[31] Y. Suzuki, N. Misawa, C. Sato, H. Ebina, T. Masuda, N. Yamamoto, Y. Koyanagi, Quantitative analysis of human immunodeficiency virus type 1 DNA dynamics by real-time PCR: integration efficiency in stimulated and unstimulated peripheral blood mononuclear cells, Virus Genes 27 (2003) 177–188.

[32] M. Huang, J.M. Orenstein, M.A. Martin, E.O. Freed, $p6^{Gag}$ is required for particle production from full-length human immunodeficiency virus type 1 molecular clones expressing protease, J. Virol. 69 (1995) 6810–6818.

[33] F. Bernassola, M. Karin, A. Ciechanover, G. Melino, The HECT family of E3 ubiquitin ligases: multiple players in cancer development, Cancer Cell 14 (2008) 10–21.

[34] D. Chen, N. Kon, M. Li, W. Zhang, J. Qin, W. Gu, ARF-BP1/Mule is a critical mediator of the ARF tumor suppressor, Cell 121 (2005) 1071–1083.

[35] Q. Zhong, W. Gao, F. Du, X. Wang, Mule/ARF-BP1, a BH3-only E3 ubiquitin ligase, catalyzes the polyubiquitination of Mcl-1 and regulates apoptosis, Cell 121 (2005) 1085–1095.

[36] R.H. Wade, A.A. Hyman, Microtubule structure and dynamics, Curr. Opin. Cell Biol. 9 (1997) 12–17.

[37] M.H. Naghavi, S.P. Goff, Retroviral proteins that interact with the host cell cytoskeleton, Curr. Opin. Immunol. 19 (2007) 402–407.

[38] V.R. de Soultrait, A. Caumont, P. Durrens, C. Calmels, V. Parissi, P. Recordon, E. Bon, C. Desjobert, L. Tarrago-Litvak, M. Fournier, HIV-1 integrase interacts with yeast microtubule-associated proteins, Biochim. Biophys. Acta 1575 (2002) 40–48.

[39] A. Ono, Relationships between plasma membrane microdomains and HIV-1 assembly, Biol. Cell 102 (2010) 335–350.

[40] R. Halwani, A. Khorchid, S. Cen, L. Kleiman, Rapid localization of Gag/GagPol complexes to detergent-resistant membrane during the assembly of human immunodeficiency virus type 1, J. Virol. 77 (2003) 3973–3984.

[41] K. Simons, D. Toomre, Lipid rafts and signal transduction, Nat. Rev. Mol. Cell Biol. 1 (2000) 31–39.

[42] E. Yung, M. Sorin, E.J. Wang, S. Perumal, D. Ott, G.V. Kalpana, Specificity of interaction of INI1/hSNF5 with retroviral integrases and its functional significance, J. Virol. 78 (2004) 2222–2231.

[43] M. Sorin, J. Cano, S. Das, S. Mathew, X. Wu, K.P. Davies, X. Shi, S.W. Cheng, D. Ott, G.V. Kalpana, Recruitment of a SAP18-HDAC1 complex into HIV-1 virions and its requirement for viral replication, PLoS Pathog. 5 (2009) e1000463.

[44] T. Izumi, A. Takaori-Kondo, K. Shirakawa, H. Higashitsuji, K. Itoh, K. Io, M. Matsui, K. Iwai, H. Kondoh, T. Sato, M. Tomonaga, S. Ikeda, H. Akari, Y. Koyanagi, J. Fujita, T. Uchiyama, MDM2 is a novel E3 ligase for HIV-1 Vif, Retrovirology 6 (2009) 1.

[45] A.L. Brass, D.M. Dykxhoorn, Y. Benita, N. Yan, A. Engelman, R.J. Xavier, J. Lieberman, S.J. Elledge, Identification of host proteins required for HIV infection through a functional genomic screen, Science 319 (2008) 921–926.

OPEN ACCESS Freely available online

PLoS one

Cloning and Characterization of the Antiviral Activity of Feline Tetherin/BST-2

Aiko Fukuma[1,2,3], Masumi Abe[2], Yuko Morikawa[3], Takayuki Miyazawa[4], Jiro Yasuda[1,2]*

1 Department of Emerging Infectious Diseases, Institute of Tropical Medicine, Nagasaki University, Nagasaki, Japan, **2** Fifth Biology Section for Microbiology, First Department of Forensic Science, National Research Institute of Police Science, Kashiwa, Japan, **3** Kitasato Institute for Life Sciences and Graduate School for Infection Control, Kitasato University, Tokyo, Japan, **4** Laboratory of Signal Transduction, Institute for Virus Research, Kyoto University, Kyoto, Japan

Abstract

Human Tetherin/BST-2 has recently been identified as a cellular antiviral factor that blocks the release of various enveloped viruses. In this study, we cloned a cDNA fragment encoding a feline homolog of Tetherin/BST-2 and characterized the protein product. The degree of amino acid sequence identity between human Tetherin/BST-2 and the feline homolog was 44.4%. Similar to human Tetherin/BST-2, the expression of feline Tetherin/BST-2 mRNA was inducible by type I interferon (IFN). Exogenous expression of feline Tetherin/BST-2 efficiently inhibited the release of feline endogenous retrovirus RD-114. The extracellular domain of feline Tetherin/BST-2 has two putative *N*-linked glycosylation sites, N79 and N119. Complete loss of *N*-linked glycosylation by introduction of mutations into both sites resulted in almost complete abolition of its antiviral activity. In addition, feline Tetherin/BST-2 was insensitive to antagonism by HIV-1 Vpu, although the antiviral activity of human Tetherin/BST-2 was antagonized by HIV-1 Vpu. Our data suggest that feline Tetherin/BST-2 functions as a part of IFN-induced innate immunity against virus infection and that the induction of feline Tetherin/BST-2 *in vivo* may be effective as a novel antiviral strategy for viral infection.

Citation: Fukuma A, Abe M, Morikawa Y, Miyazawa T, Yasuda J (2011) Cloning and Characterization of the Antiviral Activity of Feline Tetherin/BST-2. PLoS ONE 6(3): e18247. doi:10.1371/journal.pone.0018247

Editor: David Harrich, Queensland Institute of Medical Research, Australia

Received October 28, 2010; **Accepted** March 1, 2011; **Published** March 29, 2011

Funding: This work was supported by grants from the Bio-Oriented Technology Research Advancement Institution and the Japan Society for the Promotion of Science. The funders had no role in study design, data collection and analysis, decision to publish, or preparation of the manuscript.

Competing Interests: The authors have declared that no competing interests exist.

* E-mail: j-yasuda@nagasaki-u.ac.jp

Introduction

Human Tetherin/BST-2 (also referred to as CD317 or HM1.24) was first identified as a cellular restriction factor that blocks the release of HIV-1 in the absence of the viral accessory protein, Vpu [1]. Subsequent studies have shown that human Tetherin/BST-2 also inhibits the release of other retroviruses, filoviruses, arenaviruses, and herpesviruses [1–7].

Tetherin/BST-2 is a type II integral membrane protein consisting of an N-terminal cytoplasmic tail, a transmembrane domain, followed by an extracellular domain important for dimerization, and a glycophosphatidyl inositol (GPI) lipid anchor at its C-terminus [8]. The extracellular domain of Tetherin/BST-2 has two putative *N*-linked glycosylation sites, which are highly conserved at the same positions among human, rhesus monkey, dog, pig, rat, and mouse, and orthologs have been identified that are actually glycosylated heterogeneously [8,9]. Previously, we showed that *N*-linked glycosylation is dispensable for the antiviral activity of human Tetherin/BST-2 against Lassa and Marburg viruses [6]. On the other hand, there are conflicting data regarding the role of *N*-linked glycosylation on the antiviral activity of human Tetherin/BST-2 against HIV-1. Andrew *et al.* reported that *N*-linked glycosylation is not important for inhibition of HIV-1 virus release, while Perez-Caballero *et al.* showed that *N*-linked glycosylation, especially at the second site, is important for the antiviral activity of human Tetherin/BST-2 against HIV-1 [10,11].

Human Tetherin/BST-2 is constitutively expressed in terminally differentiated B cells, bone marrow stromal cells, and plasmacytoid dendritic cells, and is upregulated in various cell types on treatment with type I and type II interferon (IFN) [12,13]. Therefore, Tetherin/BST-2 is thought to be involved in antiviral host defense as an innate immunity mechanism. It has also been reported that several viruses encode antagonists, such as HIV-1 Vpu, HIV-2 Env, SIVmac/cpz/gor Nef, Ebola virus GP, and Kaposi's sarcoma-associated herpesvirus (KSHV) K5, which antagonize the antiviral activity of Tetherin/BST-2 [1,5,7,14–17].

The cat genome contains an infectious endogenous retrovirus (ERV) named RD-114 [18]. Several feline cell lines including Crandell-Rees feline kidney (CRFK) cells constitutively express infectious RD-114 [19,20]. Therefore, there is concern regarding contamination by RD-114 in vaccines, as these cells have been used to grow several live attenuated vaccines for pets and cattle. In fact, we recently reported the isolation of an infectious RD-114 in a proportion of live attenuated vaccines for pets [21]. RD-114 is considered to be a polytropic virus, since it efficiently infects feline cells as well as human and dog cells [19,22]. Although the pathogenicity of RD-114 has not been determined, it has potential risks in that interspecies transmission may induce unpredictable diseases. However, it is very difficult to completely exclude the proviral DNA of RD-114 from cells, as ERVs are usually integrated into multiple loci in the host chromosomes [18].

In this study, to investigate the potential of Tetherin/BST-2 to regulate the production of RD-114 from cells, we cloned and characterized the feline homolog of Tetherin/BST-2 and examined its ability to restrict the release of RD-114 from cells.

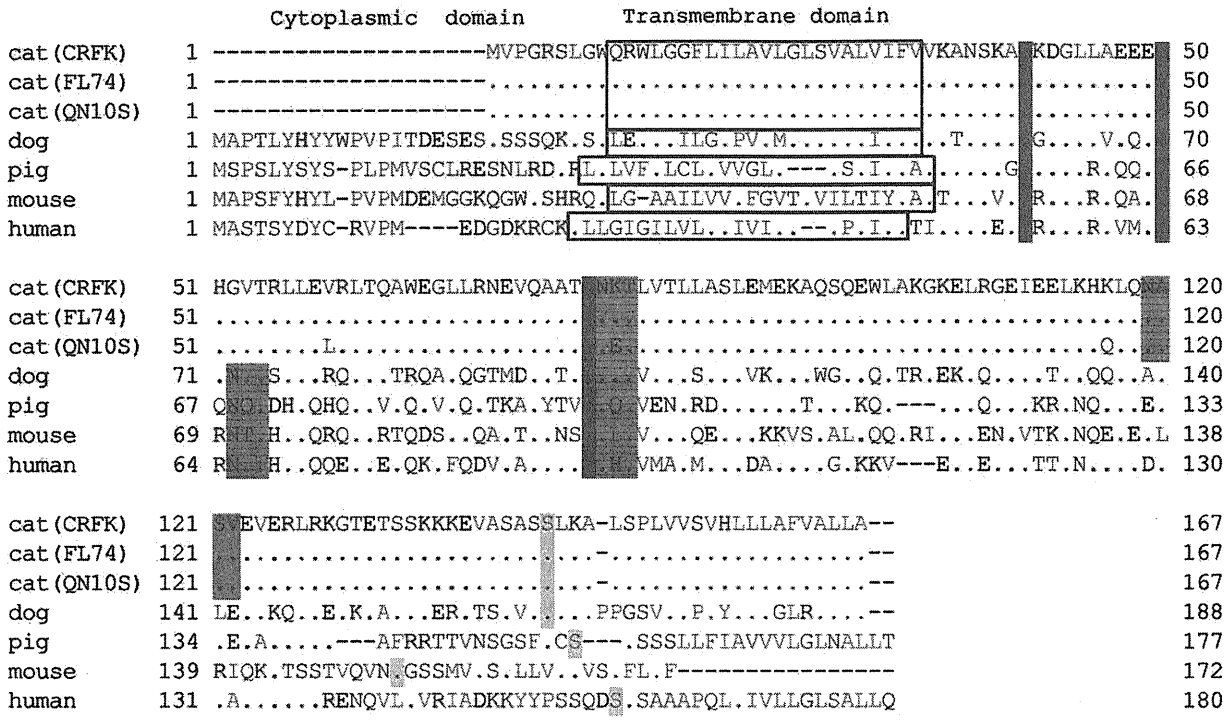

Figure 1. Comparison of the predicted amino acid sequences of cat, dog, pig, mouse, and human Tetherin/BST-2 homologs. Cat (CRFK, FL74, and QN10S cells), dog, pig, mouse, and human Tetherin/BST-2 sequences were analyzed and aligned using GENETYX ver. 8 (GENETYX, Tokyo, Japan). The predicted transmembrane domain is boxed. Three Cys residues in the extracellular domain, which are important for dimerization, are shown with a red background. Two putative glycosylation sites are shown with a blue background. Ser residues of the predicted cleavage site prior to addition of a GPI anchor are shown with a yellow background.
doi:10.1371/journal.pone.0018247.g001

Materials and Methods

Cells

Human embryonic kidney (HEK) 293T cells, Crandell-Rees feline kidney (CRFK) cells, and QN10S cells were maintained at 37°C in a 5% CO_2 incubator in Dulbecco's modified Eagle's medium (Sigma, St. Louis, MO) supplemented with 10% fetal bovine serum and penicillin/streptomycin. FL74 cells (feline T-lymphoblastoid cell line) were maintained at 37°C in a 5% CO_2 incubator in RPMI 1640 medium (Sigma) supplemented with 10% fetal bovine serum and penicillin/streptomycin.

Cloning of the feline Tetherin/BST-2 gene

The primer TethConF (5′-TCACCATCAAGGCCAACAGC-3′), corresponding to a sequence conserved among Tetherin/BST-2 genes from various species reported to date, was designed to clone feline Tetherin/BST-2. RT-PCR was performed using a PrimeSTAR RT-PCR Kit (Takara, Shiga, Japan), with total RNA extracted from IFN-treated CRFK cells as the template, according to the manufacturer's protocols. Partial cDNA fragments of feline Tetherin/BST-2 with high degrees of identity to human Tetherin/BST-2 were amplified. To determine the initiation site of the coding sequence (CDS) of feline Tetherin/BST-2, 5′-RACE was performed with a Takara 5′-Full RACE Core Set according to the manufacturer's protocols (Takara), using total RNA extracted from IFN-treated CRFK, FL74, or QN10S cells as the template. The feline Tetherin/BST-2 gene was identified. The intact CDS of feline Tetherin/BST-2 was amplified again by RT-PCR, and then cloned into pCDNFL, which was constructed from pcDNA3.1 (Invitrogen, Carlsbad, CA) to express a protein containing a FLAG-tag at the N-terminus [6,23]. The expression plasmid for feline Tetherin/BST-2 was named pfelTeth-FL.

Plasmids

The plasmids carrying human Tetherin/BST-2 or HIV-1 Vpu, pTeth-FL or pVpu-Myc, respectively, and the plasmid containing an intact infectious clone of RD-114, pTERD-114, were described previously [6,24]. The glycosylation mutants of feline Tetherin/BST-2 with asparagine to alanine substitution(s) at position 79 and/or 119, N79A, N119A, and N79A/N119A, were generated from pfelTeth-FL using a QuikChange II site-directed mutagenesis kit (Stratagene, La Jolla, CA).

Quantification of feline Tetherin/BST-2 mRNA by real-time RT-PCR

To examine the induction of feline Tetherin/BST-2 by IFN, CRFK cells were treated for 24 h in the presence of 100 or 1,000 units/ml IFN-αA/D (Sigma) and then total cellular RNA was extracted from pelleted cells using an RNeasy Mini kit (Qiagen, Valencia, CA). Real-time RT-PCR was performed using the feline Tetherin/BST-2 primers, 5′-GGAGTGTCACGGTGTCACCC-3′ (forward) and 5′-CCTCAATCTCTCCCCGAAGCTC-3′ (reverse), and the 18S rRNA primers, 5′-GACGACCCATTC-GAACGTCT-3′ (forward) and 5′-TGCTGCCTTCCTTG-GATGTG-3′ (reverse). Amplification was performed with a One-Step SYBR RT-PCR Kit (Takara) according to the manufacturer's protocols using a Smart Cycler II System (Cepheid, Sunnyvale, CA).

Assay for antiviral activity of Tetherin/BST-2 against RD-114

To examine the antiviral activity of Tetherin/BST-2, 293T cells (2×10^5) were cotransfected with pTERD-114 (100 ng) and either pTeth-FL or pfelTeth-FL (25, 50, 100, or 200 ng) using Trans-IT LT-1 (Mirus Bio Corp., Madison, WI). Forty-eight hours after transfection, virion-containing culture supernatants were clarified by centrifugation (10,000×*g*; 15 min) and virions were pelleted through a 16.5% sucrose cushion by ultracentrifugation (348,000×*g*; 40 min at 4°C). Cells were lysed with lysis buffer A [25]. Virion- and cell-associated proteins were analyzed by Western blotting using anti-RD-114 Gag antibody, anti-FLAG M2 antibody (Sigma), and anti-actin antibody (Sigma) as described previously [6,24]. The intensities of the bands for virion- and cell-associated Gag were quantified using a Fuji LAS3000 imaging system (Fuji Film, Tokyo, Japan). The control vector (virus $p28^{CA}$/virus $p28^{CA}$ + cellular $p28^{CA}$ + $p68^{Gag}$) was set to 100%. Virus production was also examined by real-time RT-PCR. Viral RNAs were extracted from pelleted virions using a QIAamp Viral RNA Mini Kit (Qiagen). After DNaseI treatment, real-time RT-PCR was performed using the previously described primers targeting the RD-114 *pol* region [26]. Amplification was performed as described above.

Results

Cloning and sequence analysis of feline Tetherin/BST-2

Molecular cloning of complete coding region of feline Tetherin/BST-2 was carried out by RT-PCR and 5′-RACE using RNA extracted from three kinds of feline cell lines, CRFK, FL74, and QN10S cells, treated with IFN. The amino acid sequences of Tetherin/BST-2 from CRFK and FL74 cells were completely identical, while that from QN10S cells was different from those from CRFK and FL74 cells at three positions, 59, 80, and 116 (Figure 1). The nucleotide sequence of the coding region of feline Tetherin/BST-2 and the corresponding protein sequence have been deposited in DDBJ (AB564550). Furthermore, Figure 1 shows the amino acid sequence alignment of Tetherin/BST-2 from cat, dog (GenBank XM_860510), pig (GenBank NM_001161755), mouse (GenBank NM_198095), and human (GenBank NM_004335). The degree of sequence identity between feline Tetherin/BST-2 and those of dog, pig, mouse, and human were 57.7%, 48.7%, 42.5%, and 44.4%, respectively. Three cysteine residues in the extracellular domain, which appear to be important for dimer formation, are conserved among all species. Two putative *N*-linked glycosylation sites are conserved at the same positions among all species other than cat. The glycosylation site in the central region of extracellular domain, N79, is conserved in feline Tetherin/BST-2, while another glycosylation site, N119, is present in the relatively C-terminal region of the extracellular domain of feline Tetherin/BST-2, but not in the region close to the transmembrane domain as in other species. We also found that the N-terminal cytoplasmic tail of feline Tetherin/BST-2 is shorter than those of other species.

Induction of feline Tetherin/BST-2 in feline cells by IFN

It has been reported that human Tetherin/BST-2 is inducible by type I IFN [1,12]. To investigate whether the expression of feline Tetherin/BST-2 is induced by type I IFN, we treated CRFK cells with 100 or 1,000 units/ml of IFN-α A/D for 24 h and determined the level of feline Tetherin/BST-2 mRNA by quantitative real-time RT-PCR. Treatment with 100 or 1,000 units/ml of IFN-α induced increases of 75- and 320-fold in feline Tetherin/BST-2 mRNA level, respectively, compared to untreated cells (Figure 2A). CRFK cells constitutively express infectious endogenous retrovirus, RD-114. IFN treatment reduced RD-114 release from CRFK cells with a concomitant increase in feline Tetherin/BST-2 expression (Figure 2B), suggesting that feline Tetherin/BST-2 inhibits release of RD-114 virus particles from cells.

Antiviral activity of feline Tetherin/BST-2 against RD-114

To directly examine whether feline Tetherin/BST-2 has inhibitory activity against RD-114 virus release, the expression plasmid for feline Tetherin/BST-2 originated from CRFK cells or human Tetherin/BST-2 was cotransfected with the RD-114 infectious clone into 293T cells and RD-114 production was analyzed by Western blotting and real-time RT-PCR assay. As shown in Figure 3A, dose-dependent reductions in RD-114 release were observed with increasing expression levels of human and feline Tetherin/BST-2. Quantitative analyses of the amounts of RD-114 virions released from cells were also carried out by Western blotting and real-time RT-PCR assay (Figure 3B and C). The inhibition of RD-114 virus release by feline Tetherin/BST-2 was demonstrated by both Western blotting and real-time RT-PCR assay. Antiviral activity of feline Tetherin/BST-2 against

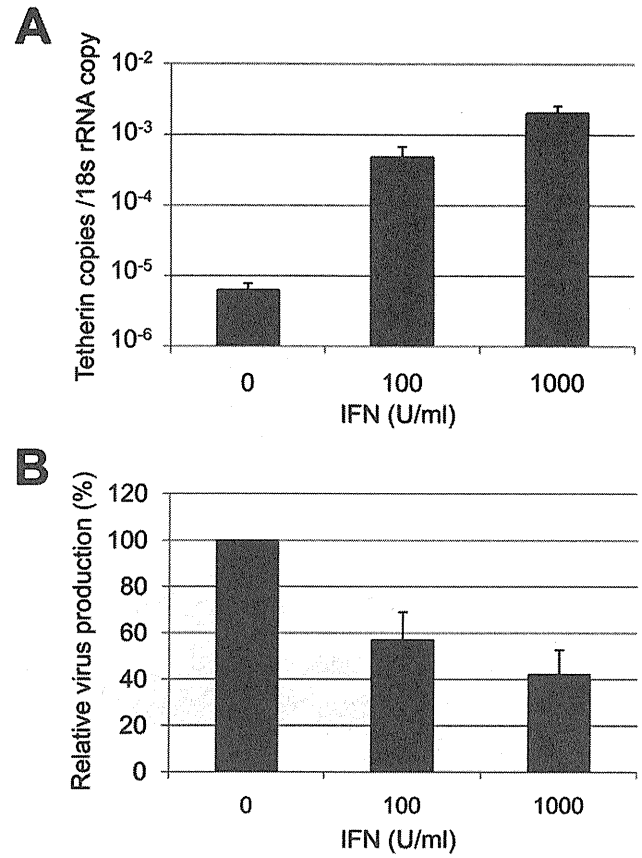

Figure 2. Induction of Tetherin/BST-2 and reduction of RD-114 particle release by IFN treatment of feline cells. CRFK cells were treated with 100 or 1,000 U/ml of IFN-α for 24 h. (A) feline Tetherin/BST-2 mRNA and 18S rRNA were quantified by real-time RT-PCR. The numbers of feline Tetherin/BST-2 mRNA copies were normalized to one copy of 18S rRNA. Histograms represent the averages from three independent experiments (± standard deviation of the mean). (B) RD-114 viral RNA in the supernatant from IFN-treated or untreated CRFK cells were quantified by real-time RT-PCR.
doi:10.1371/journal.pone.0018247.g002

RD-114 release was slightly weaker than that of human Tetherin/BST-2, although feline and human Tetherin/BST-2 were expressed at similar levels in cells transfected with the same amounts of each expression plasmid. We also confirmed that feline Tetherin/BST-2 originated from QN10S cells inhibits RD-114 production at the similar level to feline Tetherin/BST-2 originated from CRFK cells (data not shown).

Importance of *N*-linked glycosylation for antiviral activity

To examine the role of *N*-linked glycosylation of feline Tetherin/BST-2 in its antiviral function, we analyzed the effects of exogenous expression of mutants with a single or multiple mutations in the *N*-linked glycosylation sites (N79A, N119A, and N79A/N119A) on RD-114 production. 293T cells were cotransfected with the RD-114 infectious clone and increasing amounts of the expression plasmid for wild-type or mutant feline Tetherin/BST-2. Wild-type feline Tetherin/BST-2 was detected as triplet bands, while N79A and N119A mutants and N79A/N119A mutant showed double and single band(s), respectively (Figure 4), indicating that the upper, middle, and lower bands of triplet forms corresponded to multiple-, single-, and non-glycosylated forms, respectively. Exogenous expression of the N119A mutant significantly reduced RD-114 virus release as well as wild-type, while the inhibitory activity of the N79A mutant on the RD-114 virus release was lower than those of wild-type and N119A mutant despite the much higher expression level (Figure 4). Furthermore, the N79A/N119A mutant without glycosylation almost completely lost its antiviral activity. In addition, the antiviral activity of the N79A/N119A mutant could not be overcome by increased expression. These results indicated that glycosylation at N119 is not essential for the antiviral activity of feline Tetherin/BST-2, while the loss of glycosylation at N79 or at both N79 and N119 markedly affected its antiviral activity.

Feline Tetherin/BST-2 is insensitive to antagonism by HIV-1 Vpu

HIV-1 Vpu has been shown to antagonize the antiviral activity of human Tetherin/BST-2, but not monkey Tetherin/BST-2. To examine the sensitivity of feline Tetherin/BST-2 to Vpu, pVpu-Myc, which expresses Vpu containing a Myc-tag at the N-terminus, was cotransfected into 293T cells along with the RD-114 infectious clone and the expression plasmid for human or feline Tetherin/BST-2. RD-114 production was analyzed by Western blotting. As expected, Vpu expression partially rescued the RD-114 release reduction by human Tetherin/BST-2, but not that by feline Tetherin/BST-2 (Figure 5), indicating that Vpu has no effect on the antiviral activity of feline Tetherin/BST-2.

Discussion

In this study, we identified feline Tetherin/BST-2 and demonstrated the antiviral activity of feline Tetherin/BST-2.

The degree of sequence identity between feline Tetherin/BST-2 and those of dog, pig, mouse, and human were 57.7%, 48.7%, 42.5%, and 44.4%, respectively. As compared to the other cellular antiviral factors including APOBEC3 and TRIM5 proteins, the sequence homologies of Tetherin/BST-2 among mammalian species are relatively low. It has been reported that the antiviral activity of Tetherin/BST-2 require the structural features such as an N-terminal transmembrane region, a C-terminal GPI anchor, and a proper

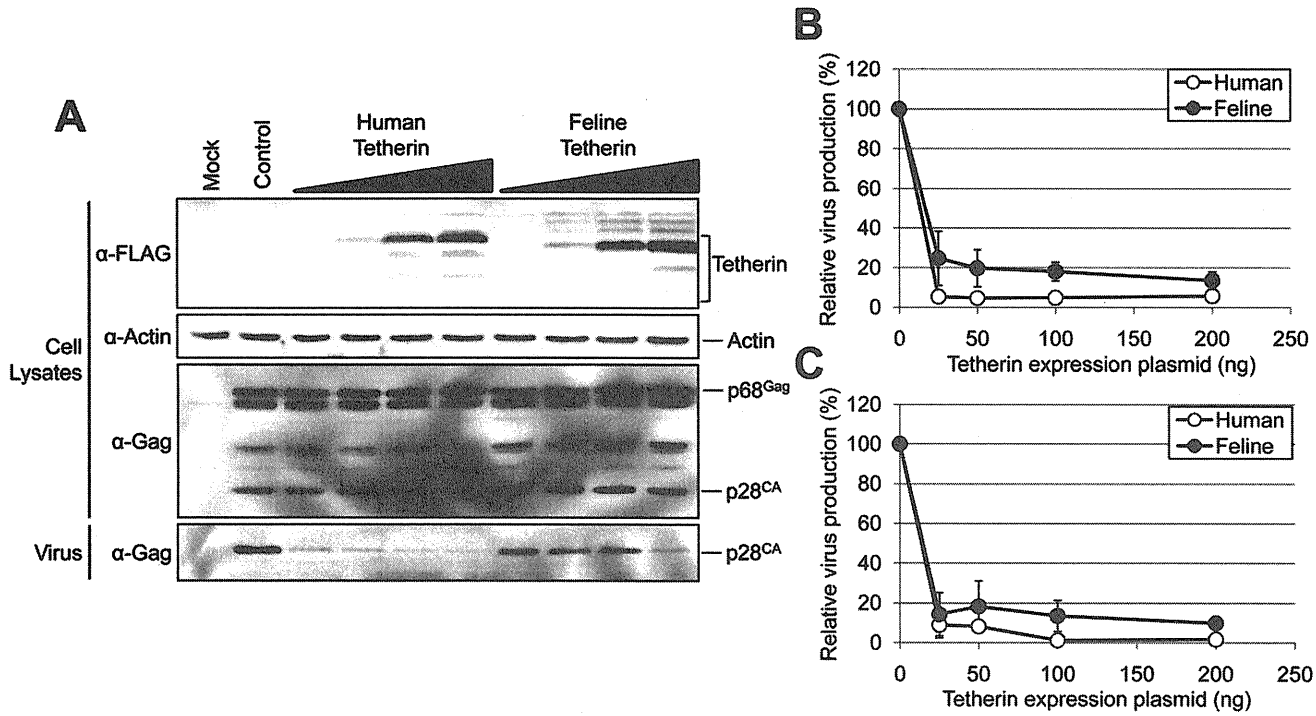

Figure 3. Inhibition of RD-114 particle release by feline Tetherin/BST-2. Both RD-114 vector (100 ng) and the expression vector for human or feline Tetherin/BST-2 containing FLAG-tag (25, 50, 100, or 200 ng) were cotransfected into 293T cells. Cells and viruses were collected at 48 h after transfection, and analyzed by Western blotting (A). The intensities of the bands for virus- and cell-associated Gag were quantified using a Fuji LAS3000 imaging system (Fuji Film) (B). The control vector (virus $p28^{CA}$/virus $p28^{CA}$ + cellular $p28^{CA}$ + $p68^{Gag}$) was set to 100%. Histograms represent the averages from three independent experiments (± standard deviation of the mean). (C) RD-114 viral RNA in the supernatant from cells was quantified by real-time RT-PCR.
doi:10.1371/journal.pone.0018247.g003

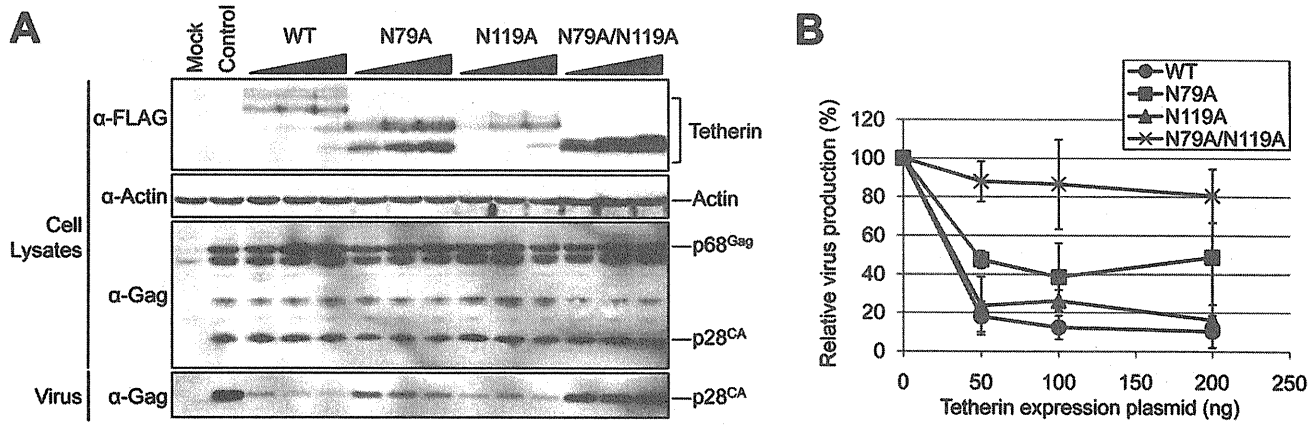

Figure 4. Importance of *N*-linked glycosylation for the antiviral activity. Both RD-114 vector (100 ng) and the expression vector for wild-type or mutant feline Tetherin/BST-2 (50, 100, or 200 ng) were cotransfected into 293T cells. Cells and viruses were collected at 48 h after transfection, and analyzed by Western blotting (A). The intensities of the bands for virus and cell-associated Gag were quantified using a Fuji LAS3000 imaging system (B). The control vector (virus $p28^{CA}$/virus $p28^{CA}$ + cellular $p28^{CA}$ + $p68^{Gag}$) was set to 100%. Histograms represent the averages from three independent experiments (± standard deviation of the mean).
doi:10.1371/journal.pone.0018247.g004

coiled-coil formation of extracellular region, but not exact amino acid sequences [11]. It would be the reason why the sequence homologies of Tetherin/BST-2 among mammalian species are relatively low.

As expected, we found that feline Tetherin/BST-2 efficiently inhibited the release of feline endogenous retrovirus RD-114 from cells, although the inhibitory effect of feline Tetherin/BST-2 against RD-114 release was slightly weaker than that of human Tetherin/BST-2 (Figure 3). RD-114 has been reported to be produced as infectious viruses in some feline cell lines and to be present as a contaminant in a proportion of live attenuated vaccines for pets [21]. It is very difficult to completely exclude the proviral DNA of RD-114 from cells, as endogenous retroviruses are usually integrated into multiple loci of the host chromosomes. The induction or exogenous expression of feline Tetherin/BST-2 in these feline cells may be useful as a novel strategy to reduce the risk of the RD-114 contamination into vaccines or biological products.

The sequence analysis of feline Tetherin/BST-2 showed that the N-terminus of feline Tetherin/BST-2 was shorter than those of other species (Figure 1). It has been reported that a dual-tyrosine motif ($Y\text{-}Y_{6-8}$) in the cytoplasmic domain of human Tetherin/BST-2 is crucial for clathrin-mediated endocytosis through recruiting AP-1 and AP-2 adaptor proteins [27,28]. Feline Tetherin/BST-2 may be internalized *via* a different pathway from the others, since feline Tetherin/BST-2 does not have this dual-tyrosine motif in its cytoplasmic domain. These features may have an effect on the weaker antiviral activity of feline Tetherin/BST-2 compared to human Tetherin/BST-2. However, at present, it is not clear whether the short cytoplasmic domain and deficiency of the dual-tyrosine motif are involved in any function of feline Tetherin/BST-2.

Although the expression levels of N79A and N79A/N119A mutants in cells were much higher than those of wild-type and N119A, the loss of glycosylation at N79, but not N119, reduced the antiviral activity of feline Tetherin/BST-2 (Figure 4). Moreover, the loss of glycosylation at both N79 and N119 almost completely inactivated the antiviral activity against RD-114. Glycosylation at N79 is conserved among Tetherin/BST-2 homologs from many species including cat (Figure 1), suggesting that this glycosylation plays an important role in the structure and function of this molecule. In addition, it has been reported previously that *N*-linked glycosylation at the corresponding site of human Tetherin/BST-2 is important for antiviral activity against HIV-1 [11]. On the other hand, glycosylation at N119 is unique in feline Tetherin/BST-2 and appears to be dispensable for the antiviral activity. Although it is not clear how glycosylation of Tetherin/BST-2 affect its antiviral activity, it has been reported that the cell surface expression levels of the glycosylation mutants of human Tetherin/BST-2 are less than that of WT [11]. The lacking of glycosylation signal may affect the intracellular transport of Tetherin/BST-2 and result in loss of the antiviral activity of Tetherin/BST-2.

HIV-1 Vpu has been reported to recognize several amino acid residues in the transmembrane domain of human Tetherin/BST-2

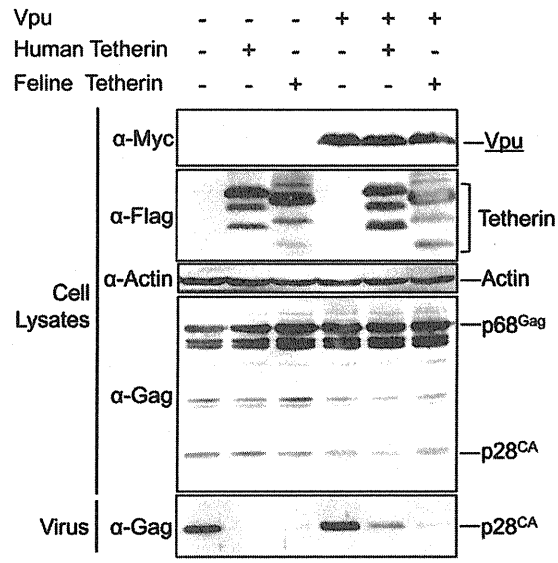

Figure 5. Feline Tetherin/BST-2 is insensitive to antagonism by HIV-1 Vpu. Both RD-114 vector (100 ng) and the expression vector for human or feline Tetherin/BST-2 containing FLAG-tag (200 ng), with or without the expression vector for Vpu containing Myc-tag (1 μg), were cotransfected into 293T cells. Cells and viruses were collected at 48 h after transfection, and analyzed by Western blotting.
doi:10.1371/journal.pone.0018247.g005

and antagonize the antiviral activity of human Tetherin/BST-2 [29,30,31]. The activity of Vpu as a Tetherin/BST-2 antagonist appears to be species specific, since Vpu inhibits the antiviral activity of human Tetherin/BST-2, but not monkey Tetherin/BST-2. In this study, we demonstrated that Vpu inhibited the reduction of RD-114 virus release by human Tetherin/BST-2, but not feline Tetherin/BST-2 (Figure 5). In addition, the cytoplasmic domain of feline Tetherin/BST-2 does not have the STS motif (at position 3-5) required for Vpu/β-TrCP-dependent ubiquitination [32]. Thus, our data support that the activity of Vpu as a Tetherin/BST-2 antagonist is specific for human Tetherin/BST-2.

Similar to human Tetherin/BST-2, the feline homolog is likely to also have antiviral activity against not only RD-114 but also a wide variety of enveloped viruses, although we demonstrated the antiviral activity of feline Tetherin/BST-2 against RD-114. In addition, we showed that the expression of feline Tetherin/BST-2 was induced by type I IFN similar to human Tetherin/BST-2 (Figure 2), suggesting that Tetherin/BST-2 functions as a host innate antiviral system against a wide variety of viruses. Analyses of the expression pattern of feline Tetherin/BST-2 *in vivo* and the mechanism of induction of Tetherin/BST-2 by IFN would be useful for understanding the specificity (tropism) of virus replication in tissues or cells and the development of antiviral strategies against a wide variety of viruses.

Acknowledgments

We thank Toshie Sakuma for plasmid preparation.

Author Contributions

Conceived and designed the experiments: AF MA YM TM JY. Performed the experiments: AF JY. Analyzed the data: AF TM YM JY. Contributed reagents/materials/analysis tools: AF MA TM JY. Wrote the paper: AF JY.

References

1. Neil SJD, Zang T, Bieniasz PD (2008) Tetherin inhibits retrovirus release and is antagonized by HIV-1 Vpu. Nature 451: 425–U421.
2. Jouvenet N, Neil SJ, Zhadina M, Zang T, Kratovac Z, et al. (2009) Broad-spectrum inhibition of retroviral and filoviral particle release by tetherin. J Virol 83: 1837–1844.
3. Mattiuzzo G, Ivol S, Takeuchi Y (2010) Regulation of porcine endogenous retrovirus release by porcine and human tetherins. J Virol 84: 2618–22.
4. Göttlinger HG, Dorfman T, Cohen EA, Haseltine WA (1993) Vpu protein of human immunodeficiency virus type 1 enhances the release of capsids produced by gag gene constructs of widely divergent retroviruses. Proc Natl Acad Sci USA 90: 7381–7385.
5. Kaletsky RL, Francica JR, Agrawal-Gamse C, Bates P (2009) Tetherin-mediated restriction of filovirus budding is antagonized by the Ebola glycoprotein. Proc Natl Acad Sci USA 106: 2886–2891.
6. Sakuma T, Noda T, Urata S, Kawaoka Y, Yasuda J (2009) Inhibition of Lassa and Marburg virus production by tetherin. J Virol 83: 2382–2385.
7. Mansouri M, Viswanathan K, Douglas JL, Hines J, Gustin J, et al. (2009) Molecular mechanism of BST2/tetherin downregulation by K5/MIR2 of Kaposi's sarcoma-associated herpesvirus. J Virol 83: 9672–9681.
8. Kupzig S, Korolchuk V, Rollason R, Sugden A, Wilde A, et al. (2003) Bst-2/HM1.24 is a raft-associated apical membrane protein with an unusual topology. Traffic 4: 694–709.
9. Ohtomo T, Sugamata Y, Ozaki Y, Ono K, Yoshimura Y, et al. (1999) Molecular cloning and characterization of a surface antigen preferentially overexpressed on multiple myeloma cells. Biochem Biophys Res Commun 258: 583–591.
10. Andrew AJ, Miyagi E, Kao S, Strebel K (2009) The formation of cysteine-linked dimers of BST-2/tetherin is important for inhibition of HIV-1 virus release but not for sensitivity to Vpu. Retrovirology. 6: 80.
11. Perez-Caballero D, Zang T, Ebrahimi A, McNatt MW, Gregory DA, et al. (2009) Tetherin inhibits HIV-1 release by directly tethering virions to cells. Cell 139: 499–511.
12. Blasius AL, Giurisato E, Cella M, Schreiber RD, Shaw AS, et al. (2006) Bone marrow stromal cell antigen 2 is a specific marker of type I IFN-producing cells in the naive mouse, but a promiscuous cell surface antigen following IFN stimulation. J Immunol 177: 3260–3265.
13. Ishikawa J, Kaisho T, Tomizawa H, Lee BO, Kobune Y, et al. (1995) Molecular cloning and chromosomal mapping of a bone marrow stromal cell surface gene, BST2, that may be involved in pre-B-cell growth. Genomics 26: 527–534.
14. Le Tortorec A, Neil SJD (2009) Antagonism to and intracellular sequestration of human tetherin by the human immunodeficiency virus type 2 envelope glycoprotein. J Virol 83: 11966–11978.
15. Zhang F, Wilson SJ, Landford WC, Virgen B, Gregory D, et al. (2009) Nef proteins from simian immunodeficiency viruses are tetherin antagonists. Cell Host Microbe 6: 54–67.
16. Sauter D, Schindler M, Specht A, Landford WN, Münch J, et al. (2009) Tetherin-driven adaptation of Vpu and Nef function and the evolution of pandemic and nonpandemic HIV-1 strains. Cell Host Microbe 6: 409–421.
17. Douglas JL, Gustin JK, Viswanathan K, Mansouri M, Moses AV, et al. (2010) The great escape: viral strategies to counter BST-2/tetherin. PLoS Pathog 6: e1000913.
18. Reeves RH, Nash WG, O'Brien SJ (1985) Genetic mapping of endogenous RD-114 retroviral sequences of domestic cats. J Virol 56: 303–306.
19. Baumann JG, Gunzburg WH, Salmons B (1998) CrFK feline kidney cells produce an RD114-like endogenous virus that can package murine leukemia virus-based vectors. J Virol 72: 7685–7687.
20. Yoshikawa R, Sato E, Igarashi T, Miyazawa T (2010) Characterization of RD-114 virus isolated from a commercial canine vaccine manufactured using CRFK cells. J Clin Microbiol 48: 3366–3369.
21. Miyazawa T, Yoshikawa R, Golder M, Okada M, Stewart H, et al. (2010) Isolation of an infectious endogenous retrovirus in a proportion of live attenuated vaccines for pets. J Viol 84: 3690–3694.
22. Dunn KJ, Yuan CC, Blair DG (1993) A phenotypic host range alteration determines RD114 virus restriction in feline embryonic cells. J Virol 67: 4704–4711.
23. Urata S, Noda T, Kawaoka Y, Yokosawa H, Yasuda J (2006) Cellular factors required for Lassa virus budding. J Virol 80: 4191–4195.
24. Sakuma T, Sakurai A, Yasuda J (2009) Dimerization of tetherin is not essential for its antiviral activity against Lassa and Marburg viruses. PLoS ONE 4: e6934.
25. Yasuda J, Hunter E (1998) A proline-rich motif (PPPY) in the Gag polyprotein of Mason-Pfizer monkey virus plays a maturation-independent role in virion release. J Virol 72: 4095–4103.
26. Sakaguchi S, Okada M, Shojima T, Baba K, Miyazawa T (2008) Establishment of a LacZ marker rescue assay to detect infectious RD114 virus. J Vet Med Sci 70: 785–790.
27. Rollason R, Korolchuk V, Hamilton C, Schu P, Banting G (2007) Clathrinmediated endocytosis of a lipid-raft-associated protein is mediated through a dual tyrosine motif. J Cell Sci 120: 3850–3858.
28. Masuyama N, Kuronita T, Tanaka R, Muto T, Hirota Y, et al. (2009) HM1.24 is internalized from lipid rafts by clathrin-mediated endocytosis through interaction with alpha-adaptin. J Biol Chem 284: 15927–15941.
29. Gupta RK, Hué S, Schaller T, Verschoor E, Pillay D, et al. (2009) Mutation of a single residue renders human tetherin resistant to HIV-1 Vpu-mediated depletion. PLoS Pathog 5: e1000443.
30. McNatt MW, Zang T, Hatziioannou T, Bartlett M, Fofana IB, et al. (2009) Species-specific activity of HIV-1 Vpu and positive selection of tetherin transmembrane domain variants. PLoS Pathog 5: e1000300.
31. Rong L, Zhang J, Lu J, Pan Q, Lorgeoux RP, et al. (2009) The transmembrane domain of BST-2 determines its sensitivity to down-modulation by human immunodeficiency virus type 1 Vpu. J Virol 83: 7536–7546.
32. Tokarev AA, Munguia J, Guatelli JC (2010) Serine-threonine ubiquitination mediates downregulation of BST-2/tetherin and relief of restricted virion release by HIV-1 Vpu. J Virol 85: 51–63.

ANTIMICROBIAL AGENTS AND CHEMOTHERAPY, Sept. 2011, p. 4251–4260 Vol. 55, No. 9
0066-4804/11/$12.00 doi:10.1128/AAC.00299-11

Novel Postentry Inhibitor of Human Immunodeficiency Virus Type 1 Replication Screened by Yeast Membrane-Associated Two-Hybrid System▽

Emiko Urano,[1,2] Noriko Kuramochi,[3] Reiko Ichikawa,[2] Somay Yamagata Murayama,[1] Kosuke Miyauchi,[2] Hiroshi Tomoda,[3] Yutaka Takebe,[2] Milan Nermut,[4] Jun Komano,[2]* and Yuko Morikawa[1]*

Kitasato Institute for Life Sciences and Graduate School of Infection Control, Kitasato University, Shirokane 5-9-1, Minato-ku, Tokyo 108-8641, Japan[1]; AIDS Research Center, National Institute of Infectious Diseases, Toyama 1-23-1, Shinjuku-ku, Tokyo 162-8640, Japan[2]; Faculty of Pharmaceutical Sciences, Kitasato University, Shirokane 5-9-1, Minato-ku, Tokyo 108-8641, Japan[3]; and National Institute for Biological Standards and Control, South Mimms, Herts EN6 3QG, United Kingdom[4]

Received 3 March 2011/Returned for modification 25 April 2011/Accepted 1 July 2011

Human immunodeficiency virus (HIV) Gag protein targets to the plasma membrane and assembles into viral particles. In the next round of infection, the mature Gag capsids disassemble during viral entry. Thus, Gag plays a central role in the HIV life cycle. Using a yeast membrane-associated two-hybrid assay based on the SOS-RAS signaling system, we developed a system to measure the Gag-Gag interaction and isolated 6 candidates for Gag assembly inhibitors from a chemical library composed of 20,000 small molecules. When tested in the human MT-4 cell line and primary peripheral blood mononuclear cells, one of the candidates, 2-(benzothiazol-2-ylmethylthio)-4-methylpyrimidine (BMMP), displayed an inhibitory effect on HIV replication, although a considerably high dose was required. Unexpectedly, neither particle production nor maturation was inhibited by BMMP. Confocal microscopy confirmed that BMMP did not block Gag plasma membrane targeting. Single-round infection assays with envelope-pseudotyped and luciferase-expressing viruses revealed that BMMP inhibited HIV replication postentry but not simian immunodeficiency virus (SIV) or murine leukemia virus infection. Studies with HIV/SIV Gag chimeras indicated that the Gag capsid (CA) domain was responsible for the BMMP-mediated HIV postentry block. *In vitro* studies indicated that BMMP accelerated disassembly of HIV cores and, conversely, inhibited assembly of purified CA protein in a dose-dependent manner. Collectively, our data suggest that BMMP primarily targets the HIV CA domain and disrupts viral infection postentry, possibly through inducing premature disassembly of HIV cores. We suggest that BMMP is a potential lead compound to develop antiretroviral drugs bearing novel mechanisms of action.

Over 2 decades, research has developed antiretroviral therapy (ART) with a combination of antiretroviral drugs for human immunodeficiency virus type 1 (HIV-1) infection (10). ART has dramatically improved the survival of HIV-1-infected individuals. Current ART involves a combination of inhibitors of HIV-specific enzymes, such as protease (PR), reverse transcriptase (RT), and integrase (IN). In some cases, inhibitors of HIV-1 entry are also used. However, the emergence of HIV-1 variants resistant to antiretroviral drugs during ART stresses the need for novel HIV-1 inhibitors against distinct targets.

Multiple screening approaches have been employed for HIV-1 drug discovery (37) and have successfully discovered HIV-1 inhibitors that are currently available: nucleoside analogue RT inhibitors were discovered by HIV replication assays (23) and PR inhibitors were produced by structure-based drug design (25). In general, cell-free assays allow discovery of compounds with a relatively low 50% effective dose (ED_{50}) *in vitro*. However, many such compounds often fail to inhibit HIV-1 replication in *in vivo* assays, because they may not penetrate the cell membrane or may easily be catalyzed in metabolic environments. Also, possible toxic effects of the compounds must be tested in a subsequent cell culture study. In contrast, cell-based screens can exclude toxic compounds but have the disadvantages of time requirements and limitations on cell propagation in high-throughput screening.

Recently, cell-based assays using engineered cells and microorganisms have become an attractive alternative to *in vitro* assays for high-throughput screening. The yeast *Saccharomyces cerevisiae* is a convenient alternative to mammalian cells for this purpose. Comparative genomic analysis has shown that approximately 30% of yeast genes have homology to the mammalian protein sequences (8), indicating that basic cellular mechanisms are well conserved between yeast and human cells. Yeast has been used as a model organism for understanding biological functions of higher eukaryotic cells, leading to accumulation of scientific knowledge in yeast genetics and molecular biology. Such pioneering research has allowed the development of molecular technologies (e.g., two-hybrid assay and galactose induction), genetically modified cells (e.g., temperature sensitivity and conditional lethality), and cell selection systems (e.g.,

* Corresponding author. Mailing address for Jun Komano: AIDS Research Center, National Institute of Infectious Diseases, Toyama 1-23-1, Shinjuku-ku, Tokyo 162-8640, Japan. Phone: 81-3-5285-1111. Fax: 81-3-5282-5037. E-mail: ajkomano@nih.go.jp. Mailing address for Yuko Morikawa: Kitasato Institute for Life Sciences and Graduate School of Infection Control, Kitasato University, Shirokane 5-9-1, Minato-ku, Tokyo 108-8641, Japan. Phone: 81-3-3444-6161. Fax: 81-3-5791-6268. E-mail: morikawa@lisci.kitasato-u.ac.jp.

▽ Published ahead of print on 11 July 2011.

URA3 nutritional selection), enabling the construction of simple readout assay systems.

Gag protein, the main structural component of retrovirus, directs particle assembly. HIV Gag protein is synthesized as a precursor protein, p55, which is composed of matrix (MA), capsid (CA), nucleocapsid (NC), and p6 domains, and cotranslationally myristoylated at the N-terminal glycine. Concomitant with the N-terminal myristoylation, p55Gag is targeted to the plasma membrane and assembled into virus particles (13, 22). During particle release, Gag undergoes proteolytic processing to generate the CA domain that forms the mature capsid. In the next round of infection, the mature capsid disassembles during viral penetration into host cell cytoplasm. Thus, the capsid assembly and disassembly are reverse reactions during virus release and entry and must be regulated by yet-unknown mechanisms. Indeed, the optimal stability of HIV-1 capsid is required for efficient infection (14). We have previously shown that the particle assembly process is reproducible in a yeast cell system (26). Here, we further developed a yeast membrane-associated two-hybrid assay system in which a temperature-sensitive mutant strain of yeast grows at restrictive temperature when Gag-Gag interactions occur. Using this yeast two-hybrid system, we have screened a chemical library composed of 20,000 low-molecular-weight compounds and have found a compound that targets CA-CA interactions and inhibits HIV-1 replication.

MATERIALS AND METHODS

Construction and transformation of yeast expression plasmids. A yeast membrane-associated two-hybrid assay based on the CytoTrap SOS recruitment system (Stratagene) was employed in this study. The full-length *gag* gene of HIV-1 (HXB2 strain) was placed downstream of the yeast inducible promoter for the *GAL1* gene in frame with the cDNA of SOS in a pSOS plasmid (Stratagene) that contains the *LEU2* gene as a yeast selective marker. The HIV-1 (HXB2 strain) *gag* gene was also cloned into pMyr plasmid, which contains a yeast inducible promoter for the *GAL1* gene and the *URA3* gene as a selective marker. The *S. cerevisiae* strain cdc25Ha (*MAT***a** *ura3-52 his3-200 ade2-101 lys2-801 trp1-901 leu2-3 112 cdc25-2* Gal^+) was doubly transformed with the yeast expression plasmids.

Chemical library screening in CytoTrap yeast membrane-associated two-hybrid system. Yeast transformants were initially grown at 25°C in synthetic defined medium with glucose (0.67% yeast nitrogen base, 2% glucose, and amino acid mixtures without uracil or leucine) (permissive conditions). After being washed, culture was diluted to an optical density at 600 nm (OD_{600}) of 0.1 in synthetic defined medium with galactose and raffinose (0.67% yeast nitrogen base, 2% galactose, 2% raffinose, and amino acid mixtures without uracil or leucine) for Gag expression. The yeast culture (OD_{600} = 0.1) was incubated with a chemical library (a final concentration of 10 μM) at 37°C for 5 days (restrictive conditions) in 96-well microtiter plates with shaking. The chemical library (preplated Diversity Set) was purchased from Enamine. After complete resuspension of cells by vortexing of microtiter plates, cell density was measured at 600 nm by a plate reader (Infinite200; Tecan).

Mammalian cells and transfection. 293T, HeLa, and MT-4 cells were provided by the AIDS Research Center, National Institute of Infectious Diseases, Japan. 293FT cells were purchased from Invitrogen. Peripheral blood monocytic cells (PBMC) were isolated by Ficoll-Conray density centrifugation from healthy donors. All mammalian cells were maintained in RPMI 1640 medium (Sigma) supplemented with 10% fetal bovine serum (Japan Bioserum, Japan), 100 U/ml penicillin, and 100 mg/ml streptomycin (Invitrogen), at 37°C in a humidified 5% CO_2 atmosphere. For PBMC culture, GlutaMax-I (Invitrogen), insulin-transferrin-selenium A (Invitrogen), 200 ng/ml anti-CD3 monoclonal antibody (OKT3; Janssen Pharmaceutical), and 70 U/ml recombinant human interleukin-2 (IL-2; Shionogi Pharmaceutical, Japan) were further added to the medium. Transfection was carried out with Lipofectamine 2000 according to the manufacturer's protocol (Invitrogen).

Cell toxicity assays. For determining the toxicity of the chemical library to yeast, yeast cultures were diluted to an OD_{600} of 0.01 and incubated under permissive conditions (at 25°C in glucose medium) with the chemical library. After 2 days, cell density was measured at 600 nm by a plate reader (Infinite200; Tecan). For determining toxicity to mammalian cells, 293T, 293FT, HeLa, and MT-4 cells and PBMC were incubated with compounds at 37°C for 2 to 14 days and subjected to 3-(4,5-dimethylthiazol-2-yl)-5-(3-carboxymethoxyphenyl)-2-(4-sulfophenyl)-2H-tetrazolium (MTS) and Alamar Blue assays according to the manufacturer's instructions. The OD of the MTS assay mixture was measured at 490 nm, and the OD of the Alamar Blue assay mixture was measured at 570 nm by a plate reader (FLx800; BioTek). The 50% cytotoxicity concentrations were defined as drug concentrations by which the OD values reached the 50% level of the no-drug (dimethyl sulfoxide [DMSO]) controls.

HIV-1 replication assays. MT-4 Luc cells that were transduced with luciferase in MT-4 cells (31) and PBMC were grown in RPMI 1640 medium supplemented with 10% fetal bovine serum. MT-4 Luc cells were infected with HIV-1 (HXB2 strain) corresponding to 1.25 ng of p24CA antigen and incubated at 37°C in the presence of compounds. On day 7, MT-4 Luc cells were subjected to luciferase assay. PBMC were stimulated with IL-2 and anti-CD3 antibody. Following infection with HIV-1 (HXB2 strain) corresponding to approximately 5 ng of p24CA antigen, PBMC were incubated at 37°C and passaged every 3 to 4 days in the presence of compounds. The culture supernatants of PBMC were temporally collected and subjected to quantification of HIV-1 particle yields by p24CA antigen capture enzyme-linked immunosorbent assay (ELISA; Zeptometrix).

Single-round infection assays. For single-round infection assays, HIV-1 was pseudotyped with either HIV-1 Env protein or vesicular stomatitis virus (VSV) G protein as described previously (35). Briefly, 293FT cells were transfected with a plasmid containing the codon-optimized HXB2 *gag-pol* gene (pHIVgag-pol), a lentiviral plasmid expressing luciferase (pLenti-luciferase), a plasmid expressing HIV-1 Rev (pRevpac), and either a plasmid expressing HIV-1 Env or a plasmid expressing VSV-G. Culture media were harvested and inoculated into MT-4 and 293FT cells in the presence of 5 to 10 μg/ml dextran (ICN). HIV-1 pseudotyped with autologous HIV-1 Env protein was inoculated into 293FT-CD4 (expressing CD4 constitutively) cells. On day 2 or 3, infectivity was assessed by luciferase activity transduced by pLenti-luciferase. HIV-1 (NL43 strain) expressing luciferase, simian immunodeficiency virus (SIV) (mac239 strain), and murine leukemia virus (MLV) (Moloney strain) were similarly pseudotyped with VSV-G (28). The viruses were enriched by centrifugation through sucrose cushions if necessary.

HIV/SIV Gag chimeras were generated in the context of pHIVgag-pol by replacing the MA and CA domains with the SIV MA and CA domains, respectively. The Gag chimeras contain the cleavage site sequences of HIV-1 Gag at the chimera junctions. Amino acid substitutions G89A and P90A in the cyclophilin A (CypA)-binding loop of CA (corresponding to Gag amino acid positions 225 and 226) (11, 16) were carried out by overlap PCR in the context of pHIVgag-pol.

Quantitative PCR for HIV-1 cDNA synthesis. MT-4 cells were infected with HIV-1 (HXB2 strain) and incubated in the presence of compounds. Efavirenz (EFV) was provided by the NIH AIDS Research and Reference Reagent Program and was used as positive control. The cellular genomic DNA was extracted 4 and 24 h postinfection with a DNeasy kit (Qiagen) according to the manufacturer's instructions. The cellular DNA was subjected to quantitative real-time PCR using the Quantitec probe PCR kit containing SYBR green (Qiagen). The following primer sets were used: 5′-AACTAGGGAACCCACTGCTTAAG-3′ and 5′-CTGCTAGAGATTTTCCACACTGAC-3′ (specific for the R-U5 region in early reverse transcripts of HIV-1 cDNA), 5′-CCGTCTGTTGTGTGACTC TGGT-3′ and 5′-GAGTCCTGCGTCGAGAGAGCT-3′ (specific for the late reverse transcripts of HIV-1 cDNA), 5′-TGCTGGGATTACAGGCGTGAG-3′ and 5′-CTGCTAGAGATTTTCCACACTGAC-3′ (specific for long terminal repeat [LTR] and *Alu* region in the integrated HIV-1 cDNA), and 5′-AACTAG GGAACCCACTGCTTAAG-3′ and 5′-CTGCTAGAGATTTTCCACACTGA C-3′ (second PCR) (specific for LTR region in the integrated HIV-1 cDNA) (12). The amplification kinetics was monitored by the Opticon 2 system (Bio-Rad). The levels of cellular DNA were normalized by the levels of β-globin DNA quantified using primers 5′-TATTGGTCTCCTTAAACCTGTCTTG-3′ and 5′-CTGACACAACTGTGTTCACTAGC-3′ (19).

Viral protein expression and particle purification. HIV-1 proviral clone pHXB2 was transfected into 293FT and HeLa cells in the presence of increasing doses of 2-(benzothiazol-2-ylmethylthio)-4-methylpyrimidine (BMMP). After 2 days, cells were analyzed by Western blotting using anti-HIV-1 p24CA monoclonal antibody (100-fold diluent of 183-H12-5C hybridoma culture supernatant; NIH AIDS Research and Reference Reagent Program). HIV particles were collected by centrifugation through 20% (wt/vol) sucrose cushions in an SW55

rotor (Beckman Coulter) at 120,000 × *g* for 1 h. For HIV/SIV Gag chimeras, 293FT cells were cotransfected with pHIVgag-pol expressing Gag chimera, pLenti-luciferase, pRevpac, and a plasmid expressing VSV-G. Cells and purified particles were similarly analyzed by Western blotting using anti-HIV-1 p24CA, anti-HIV-1 p17MA (2 μg/ml; 13-103-100; Advanced Biotechologies), and anti-SIV p27CA (1 μg/ml; 4324; Advanced Bioscience Laboratories) monoclonal antibodies.

***In vitro* assembly reaction of CA.** The *in vitro* assembly reaction of CA was performed as described previously (17, 36). Briefly, the purified HIV-1 CA (a final concentration of 100 μM) was incubated at 37°C for 1 h in buffer containing 20 mM Tris (pH 8.0), 500 mM NaCl, 0.2 mM EDTA, and 1 mM dithiothreitol. Assembly products were pelleted by centrifugation at 18,000 × *g* for 30 min at 4°C and were subjected to p24CA antigen capture ELISA (Zeptometrix) and electron microscopy.

***In vitro* disassembly reaction of capsid cores.** The *in vitro* disassembly assay was performed according to Aiken's method with some modifications (3). HIV particles were purified by ultracentrifugation through 20% (wt/vol) sucrose cushions. For isolation of HIV capsid cores, purified HIV particles were applied onto sucrose step gradients composed of 7.5% (wt/vol), 15% (wt/vol) containing 1% Triton X-100, and 30 to 70% (wt/vol) sucrose and subjected to centrifugation at 120,000 × *g* for 16 h at 4°C. Fractions rich in HIV cores were collected and resuspended in buffer (10 mM Tris [pH 7.4], 100 mM NaCl, and 1 mM EDTA). For core disassembly assays, aliquots of HIV cores were incubated at 37°C in the presence of compounds. For comparison, azidothymidine (AZT) (Moravek Biochemicals) was added to the reaction mixture. Intact cores were recovered by centrifugation at 125,000 × *g* for 30 min at 4°C.

Confocal microscopy and electron microscopy. HeLa cells were transfected with a pNL43 derivative expressing Gag-green fluorescent protein (GFP) fusion protein but not *pol* gene products. Cells were fixed with 3.7% paraformaldehyde in phosphate-buffered saline (PBS) for 30 min at room temperature and were treated with 0.1% Triton X-100 for 10 min at room temperature for membrane permeabilization. Following nuclear staining with TO-PRO-3 (Molecular Probes), cells were mounted with antibleaching reagent and observed with a laser scanning microscope (TCS; Leica).

In vitro assembly products were adsorbed onto carbon-coated copper grids and stained with 2% (wt/vol) uranyl acetate. Sections were subjected to electron microscopy.

Statistical analysis. Intergroup comparisons were performed with paired *t* test (for parametric group analysis). All *P* values were considered significant if less than 0.05.

RESULTS

A yeast membrane-associated two-hybrid system for HIV-1 Gag-Gag interactions. For construction of a yeast cell-based Gag assembly system, we employed a yeast membrane-associated two-hybrid assay based on the CytoTrap SOS recruitment system (Stratagene) in this study (Fig. 1). For HIV-1 Gag expression, two yeast expression plasmids, pMyr and pSOS, were used: pMyr contains the yeast inducible promoter for the *GAL1* gene followed by a myristoylation signal (amino acid sequence, MGSSKSKPKDPSQRR) for membrane targeting and pSOS contains the constitutive promoter for the yeast *ADH* gene followed by the human SOS gene. The *gag* gene of HIV-1 (HXB2 strain) was cloned in frame with the myristoylation signal in pMyr. The *gag* gene was similarly cloned in frame with the SOS gene in pSOS that allowed production of SOS-Gag fusion protein (Fig. 1A). The *S. cerevisiae* cdc25H strain was doubly transformed with these Gag expression plasmids. The cdc25H strain contains a temperature-sensitive mutation in the CDC25 gene, which allows growth at 25°C (permissive temperature) but not at 37°C (restrictive temperature). SOS is the human orthologue of the yeast CDC25 and can activate the yeast RAS signal transduction pathway that complements the yeast *cdc25* defect (4). When myristoylated Gag and SOS-Gag are coexpressed in the cdc25H cells, the SOS-Gag is recruited to the plasma membrane through an interaction with the myristoylated Gag, leading to growth of the cdc25H cells at 37°C (Fig. 1B). We initially confirmed that the cdc25H cells transformed with the Gag/pMyr and Gag/pSOS plasmids grew at 37°C in galactose plus raffinose medium under conditions in which SOS-Gag fusion protein was expressed but not at 37°C in glucose medium under conditions in which SOS-Gag fusion was not expressed.

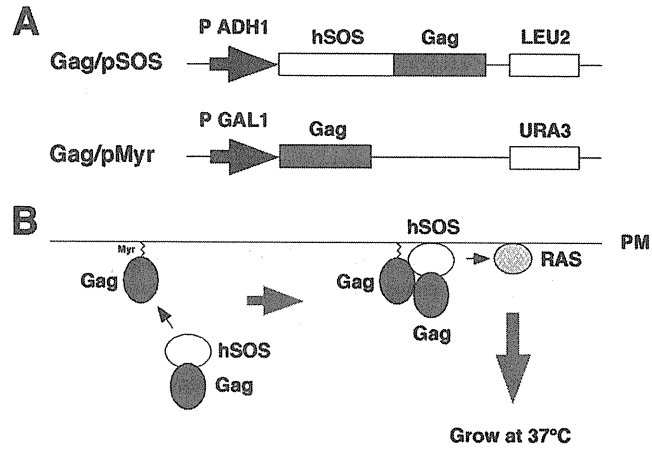

FIG. 1. Yeast membrane-associated two-hybrid screening for inhibitors of Gag-Gag interaction. (A) Schematic representation of Gag expression plasmids used for yeast SOS recruitment system. The full-length *gag* gene of HIV-1 (HXB2 strain) was expressed by yeast expression plasmids pMyr and pSOS: pMyr contains the yeast inducible promoter for the *GAL1* gene and the *URA3* gene as a selective marker and pSOS contains the constitutive promoter for the yeast *ADH* gene and the *LEU2* gene as a selective marker. (B) Principle of yeast membrane-associated two-hybrid assay based on SOS recruitment system. The schematic illustration was adapted with permission from the manuals for the CytoTrap yeast system (Agilent Technologies, Inc.; http://www.genomics.agilent.com/CollectionSubpage.aspx?PageType=Product&SubPageType=ProductDetail&PageID=1311).

Screening of a chemical library for Gag-Gag interaction inhibitors by yeast membrane-associated two-hybrid assays. For screening for inhibitors of Gag assembly, we optimized this yeast membrane-associated Gag-Gag interaction system to a liquid format using 96-well microplates. Using this system, we screened a chemical library composed of 20,000 compounds, each of which was initially designated by the numbers of microplates and wells of the chemical library (e.g., 172A6 indicates microplate number 172 and well number A6). When the cdc25H transformant was incubated at 37°C in galactose plus raffinose medium with a chemical library (10 μM each), we found 10 compounds that reduced cell growth (Fig. 2A, black columns). To examine if cell growth reduction is specifically due to the disruption of Gag-Gag interaction, we used another cdc25H transformant that contained MAFB/pSOS and SOS binding protein/pMyr plasmids. This combination produces SOS-MAFB fusion protein and myristoylated SOS binding protein and can be used as a positive control for the CytoTrap system (Stratagene). When using this positive control, we observed that 4 compounds (2G5, 73A7, 189A9, and 235C2) out of the 10 compounds also reduced cell growth (Fig. 2A, white columns), suggesting that they might inhibit pathways which are commonly used in the CytoTrap system (e.g., N myristoylation and RAS signaling). Thus, we concluded that 6 compounds (1G5, 31E7, 34A8, 73A5, 147B2, and 172A6) specifi-

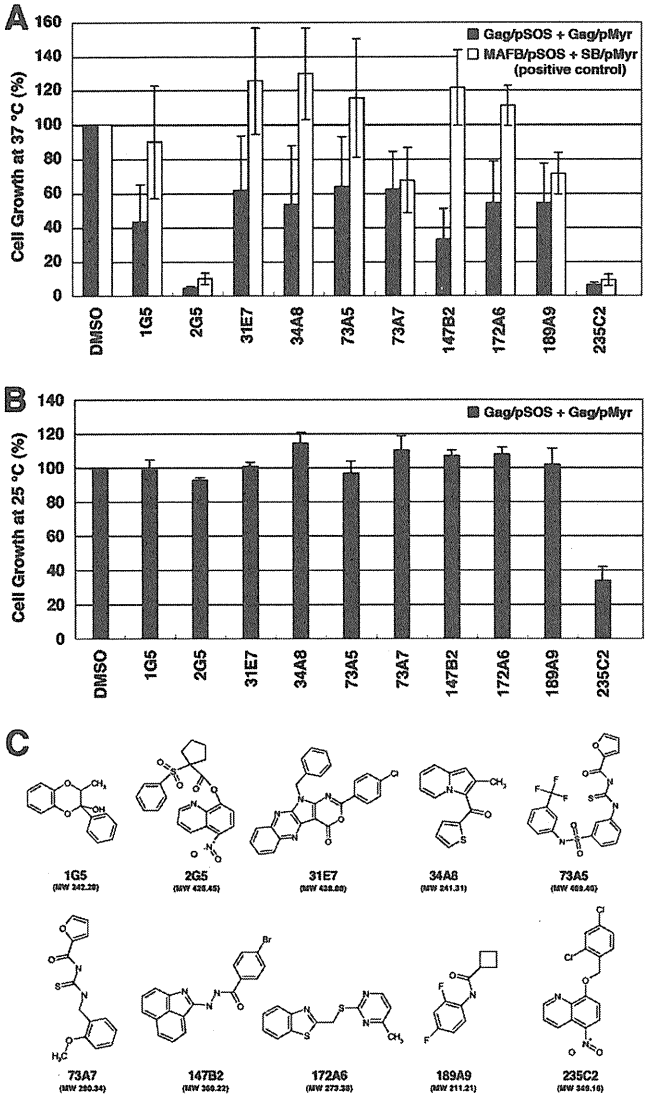

FIG. 2. Screening for inhibitors of Gag assembly by yeast membrane-associated two-hybrid assays. (A) The yeast cdc25Ha strain was transformed with the pSOS and pMyr plasmids. The yeast culture was diluted to an OD_{600} of 0.1 and incubated at 37°C in galactose-plus-raffinose medium (restrictive conditions) with a chemical library (a final concentration of 10 μM). After growth at 37°C for 5 days, cell density was measured at OD_{600}. As a control, the OD_{600} of yeast incubated in the presence of DMSO was set to 100%. The yeast transformed with the pSOS and pMyr plasmids, both of which contained the HIV-1 *gag* gene, was shown as black columns, and the yeast was transformed with the pSOS plasmid containing MAFB and the pMyr plasmid containing the cDNA of SB (as a positive-control combination) as white columns. Data were shown as means with standard deviations from 5 independent experiments. (B) The yeast cdc25Ha strain transformed with the pSOS and pMyr plasmids containing the HIV-1 *gag* gene was grown at 25°C in glucose medium. The yeast culture was diluted to an OD_{600} of 0.01 and incubated at 25°C in glucose medium with a chemical library (a final concentration of 10 μM). After growth at 25°C for 2 days, cell density was measured at OD_{600}. As a control, the OD_{600} of yeast incubated in the presence of DMSO was set to 100%. Data were shown as means with standard deviations from 3 independent experiments. (C) Structures of compounds screened from a chemical library by yeast membrane-associated two-hybrid assays.

cally inhibited a Gag-Gag interaction. No common chemical structures were found among the 6 candidates. However, 3 chemicals (34A8, 147B2, and 172A6) share relatively similar structures whereby two allyl groups are connected by a short linker moiety. To test the cell toxicity, the cdc25H transformants were incubated at 25°C in glucose medium (permissive conditions) with the compounds (10 μM each) (Fig. 2B). All the compounds except 235C2 allowed cell growth at levels comparable to that obtained in the presence of DMSO (as a control). Further studies revealed that 235C2 preferentially inhibited growth of several fungi *in vitro* (e.g., *Candida albicans* and *Aspergillus fumigatus* at MICs of 5.7 and 10 μM, respectively) (data not shown), suggesting that it might serve as a lead compound to develop an antifungal agent. The chemical formulas of 10 compounds are shown in Fig. 2C.

Inhibition of HIV replication in mammalian cells by compounds identified as yeast membrane-associated Gag-Gag interaction inhibitors. We evaluated the anti-HIV activity of the 6 candidates in mammalian cell systems. MT-4 Luc cells (human T lymphocytic cell line expressing luciferase constitutively) were infected with HIV-1 (HXB2 strain) and incubated at 37°C in the presence of the test compounds. In this T cell system, the luciferase activity is reduced by HIV-1 infection, due to the cell death upon HIV-1 replication (31). When added to HIV-1-infected MT-4 Luc cells, one of the candidates (172A6) recovered the luciferase expression in a dose-dependent manner (Fig. 3A), indicating that 172A6 was capable of reduction in HIV replication in mammalian cells. When 293T cells were incubated with the 6 compounds and were subjected to Alamar Blue assays, none of the compounds showed apparent reduction in cell viability (Fig. 3B). To confirm the anti-HIV effect, PBMC were infected with HIV-1 in the presence of 172A6 and production of HIV in the culture medium was temporally measured by p24CA antigen capture ELISA. 172A6 limited HIV replication at 5 μM and severely inhibited it at 25 μM (Fig. 3C, upper panel). When uninfected PBMC were similarly exposed to 172A6 and assessed by MTS assays, a slight reduction in cell viability was observed at 25 μM (Fig. 3C, lower panel). However, the severe inhibition of HIV replication at 25 μM 172A6 could not be ascribed fully to its cytotoxic effect. Using several mammalian cell lines, we reevaluated cytotoxicity of 172A6 by MTS assays. No significant cytotoxicity of 172A6 was seen in the cell lines, except in PBMC, that we used in this study (Fig. 3D). Based on the chemical structure [2-(benzothiazol-2-ylmethylthio)-4-methylpyrimidine] of the compound 172A6 (Fig. 2C), we called it BMMP here.

No inhibition of HIV particle release by BMMP. We initially examined whether BMMP inhibited HIV-1 particle production. 293FT cells were transfected with pHXB2 and incubated at 37°C in the presence of 5 to 50 μM BMMP. Western blotting using anti-HIV-1 p24CA antibody revealed that the intracellular level of Gag expression and the pattern of Gag processing were largely unaffected in the presence of BMMP (Fig. 4A), suggesting that BMMP did not inhibit HIV protease. When purified particle fractions were similarly analyzed, we found no reduction in particle production (Fig. 4A). We obtained similar results on HeLa cells. This indicates that BMMP did not block HIV-1 particle release.

Intracellular distribution of Gag was examined by confocal

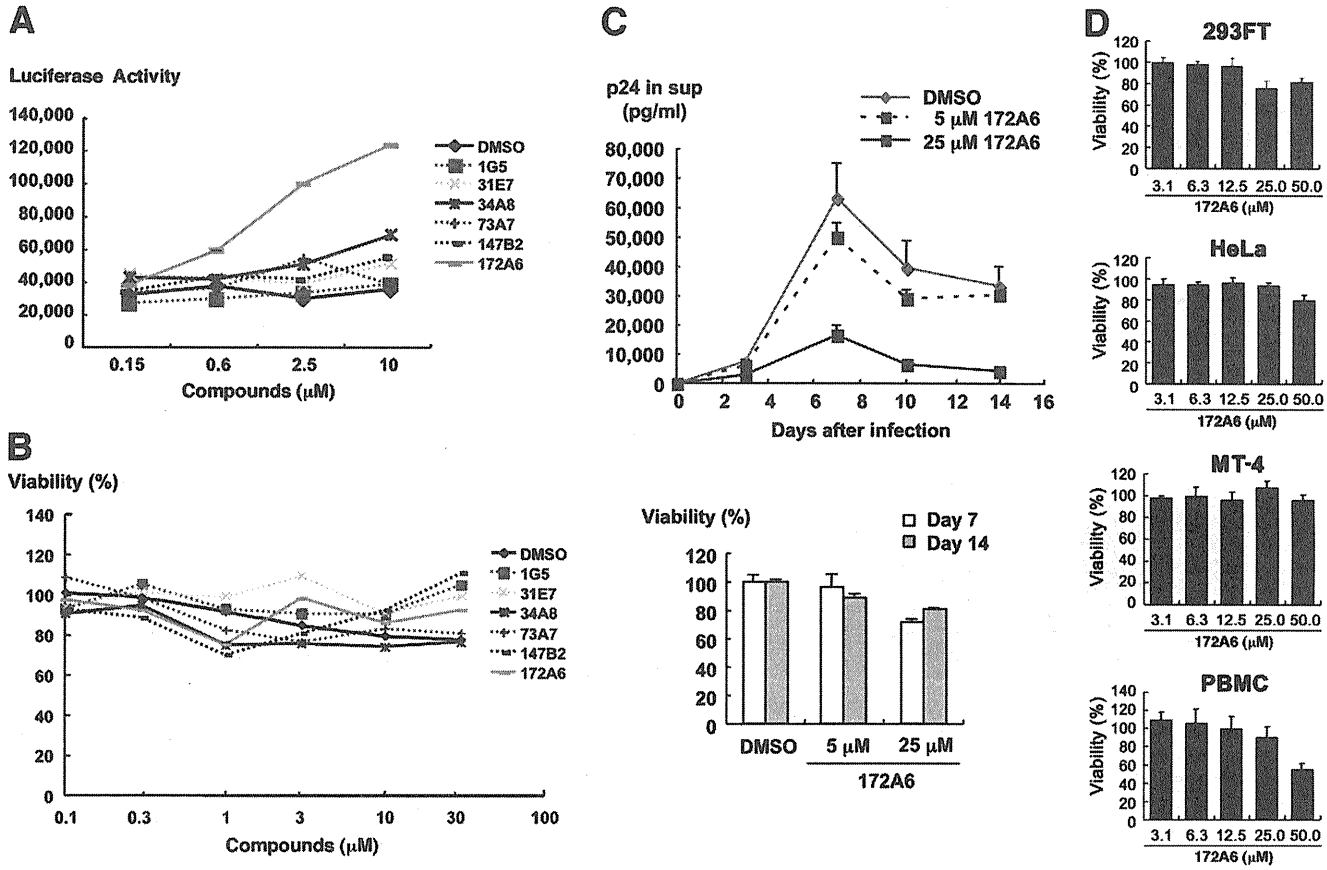

FIG. 3. Inhibition of HIV-1 replication and cell toxicity. (A) MT-4 Luc cells were infected with HIV-1 (HXB2 strain) and incubated at 37°C in the presence of increasing doses of compounds. On day 7, MT-4 Luc cells were subjected to luciferase assay. Data were shown as means from triplicate cultures. (B) 293T cells were incubated with various doses of compounds at 37°C for 2 days and subjected to Alamar Blue assays. Data were shown as means from 3 independent experiments. (C) PBMC stimulated with IL-2 and anti-CD3 antibody were infected with HIV-1 (HXB2 strain) and incubated at 37°C in the presence of 5 and 25 μM 172A6. HIV-1 production in culture medium was temporally quantified by p24CA antigen capture ELISA (top). Uninfected PBMC were cultured with 172A6 at 37°C and were subjected to MTS assay on days 7 and 14. Data were shown as means with standard deviations from triplicate cultures, in which DMSO was used as control. (D) 293FT, HeLa, and MT-4 cells and PBMC were incubated at 37°C with various doses of 172A6 and were subjected to MTS assay on days 4, 3, 4, and 6, respectively. Cell viability was shown as OD_{490}. Data were shown as means with standard deviations from triplicate cultures.

microscopy (Fig. 4B). HeLa cells were transfected with a pNL43 derivative that expresses Gag-GFP and incubated with 30 μM BMMP. Gag-GFP was distributed predominantly at the plasma membrane in cells treated with DMSO (used as control). A similar Gag-GFP distribution was observed in cells treated with BMMP, indicating that BMMP did not inhibit Gag targeting to the plasma membrane, consistent with the above findings.

Inhibition of HIV replication postentry by BMMP. To examine whether BMMP exerted an inhibitory effect on early stages of the HIV life cycle, such as viral entry, we employed single-round infection assays with luciferase-expressing HIV-1 vectors which were pseudotyped with either VSV-G or authentic HIV-1 Env protein. To this end, pHIVgag-pol (for expression of HIV-1 Gag and Gag-Pol), pRevpac (for expression of HIV-1 Rev), and pLenti-luciferase vector, which provides the artificial lentiviral genome expressing luciferase driven by cytomegalovirus promoter, were cotransfected with either VSV-G or authentic HIV-1 Env expression plasmid into 293FT cells. HIV-1 Luc viruses produced were inoculated into MT-4 cells in the presence of BMMP, and viral infectivity was monitored by a luciferase reporter assay. Luciferase expression was inhibited in a BMMP dose-dependent manner in cells infected with the HIV-1 Env-pseudotyped Luc virus, indicating that BMMP inhibited the early stage of the HIV-1 life cycle (Fig. 5A). However, when VSV-G-pseudotyped Luc virus was used, a dose-dependent reduction was similarly observed. When HIV-1 (NL43 strain) expressing luciferase was pseudotyped with VSV-G and used in this assay, the luciferase activity driven by the LTR promoter was similarly reduced in the presence of BMMP, suggesting that BMMP did not inhibit the stage of HIV entry (e.g., attachment and membrane fusion processes) but the stage of postentry (e.g., uncoating) (Fig. 5A). The Env-independent infectivity reduction was confirmed when HIV-1 Luc viruses were inoculated into 293FT and 293FT-CD4 cells (Fig. 5B). We examined whether BMMP also blocked the postentry stage of SIV. Interestingly, single-round infection assays with luciferase-expressing SIVmac239 vectors which were pseudotyped with VSV-G protein showed no inhibition of luciferase expres-

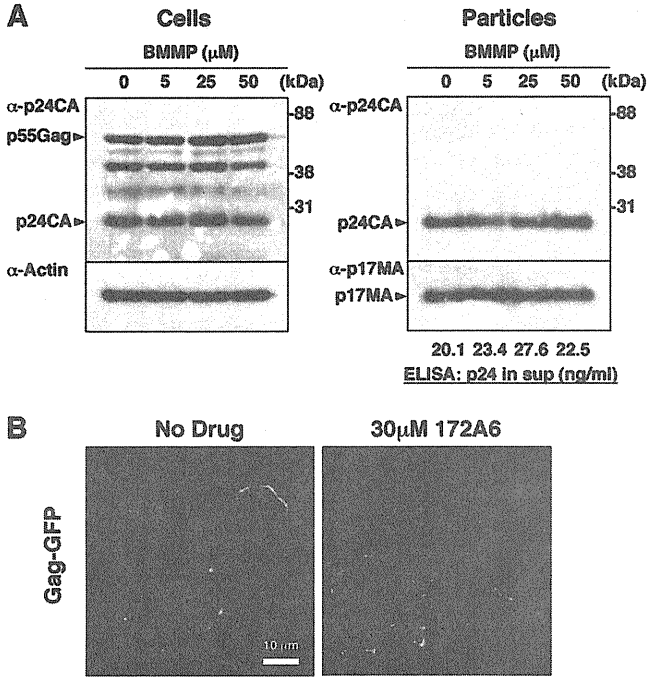

FIG. 4. HIV-1 particle production and Gag plasma membrane targeting. (A) Effects on HIV-1 particle production. 293FT cells were transfected with pHXB2 and incubated at 37°C with 0 to 50 μM BMMP. Two days posttransfection, cells were collected and culture media were subjected to purification of viral particles by ultracentrifugation. Equivalent volumes of samples were subjected to SDS-PAGE followed by Western blotting using anti-HIV-1 p24CA antibody. Representative blots were shown. HIV-1 particle yields in culture media were quantified by p24CA antigen capture ELISA. (B) Intracellular localization of Gag. HeLa cells were transfected with a pNL43 derivative in which Gag was fused with GFP and incubated at 37°C for 1.5 days with 30 μM BMMP. Nuclei were stained with TO-PRO-3, and cells were observed by confocal microscopy. Representative images were shown at the same magnification. Bar = 10 μm.

sion (Fig. 5B). No reduction in luciferase expression was also observed when luciferase-expressing pseudotyped MLV was used (data not shown). These data suggest that BMMP specifically inhibits HIV replication postentry but not those of other retroviruses, such as SIV and MLV.

To confirm the postentry block prior to particle production, we isolated cellular DNA from MT-4 cells infected with HIV-1 (HXB2 strain) that were treated with BMMP. Then, we quantified early reverse transcripts of HIV (corresponding to the strong-stop DNA), late reverse transcripts of HIV, and integrated HIV DNA by PCR. When normalized to the level of β-globin DNA (internal control), the levels of the early and late reverse transcripts and of the integrated proviral DNA were reduced, as observed for cells treated with 200 nM efavirenz controls (Fig. 5C). However, RT enzymatic activity was not affected by BMMP when examined in *in vitro* assays (data not shown). Together, these data indicate that BMMP blocks the early stage of the HIV-1 life cycle, preventing the completion of reverse transcription.

Mapping of Gag domain targeted by BMMP. To map the HIV Gag domain responsible for the postentry block by BMMP, a series of chimeric Gag constructs between HIV-1 and SIVmac239 were made in the context of pHIVgag-pol. HIV-1 MA, MACA, and CA were replaced by SIV MA, MACA, and CA, respectively (referred to as sMA, sMACA, and sCA, respectively). These Gag/Gag-Pol expression plasmids were cotransfected with pRevpac and pLenti-luciferase vector, and viruses were pseudotyped with VSV-G protein. Western blotting using anti-HIV-1 p17MA and p24CA and anti-SIVmac p27CA antibodies revealed that, although the anti-HIV-1 p24CA antibody that we used was cross-reactive with SIV CA, each domain of Gag was replaced in the chimeric constructs and virus particles were produced at levels largely similar to that of the wild type of HIV-1 Gag construct (Fig. 6A). Single-round infection assays with these Gag chimeras revealed that BMMP inhibited viral infection postentry only when HIV-1 CA was present in the constructs (Fig. 6B). Thus, our data indicated that BMMP inhibited the early stage of HIV-1 replication in a CA-specific and species-specific manner. These phenotypes resemble those observed for the CA-specific retroviral restriction imposed by a host factor, tripartite motif protein 5 (TRIM5) (30). HIV-1 CA is known to bind a host factor, CypA, likely through amino acids G89 and P90 in the exposed loop of CA (15, 16). This binding facilitates the early stage of HIV-1 replication prior to reverse transcription (9). Interestingly, HIV/SIV chimera studies have shown that the CypA-binding site overlaps with the determinants for species-specific restriction (30, 34). Thus, we made an HIV-1 Gag construct containing amino acid substitutions G89A and P90A in the CypA-binding loop of CA (referred to as CypA mt) and tested the sensitivity to BMMP. The CypA mt did not display the resistance to BMMP (Fig. 6B), suggesting that HIV-1 inhibition by BMMP was not linked to the CypA binding or TRIM5. No firm conclusions were drawn from mapping experiments using Gag chimeras within CA, i.e., N- and C-terminal domains (NTD and CTD), since the CTD mutant showed a lower yield of particle production (data not shown).

Disassembly of HIV capsid core by BMMP. The chimera experiments showed that the CA domain is critical for the inhibitory effect of BMMP on the early stage of HIV-1 replication. Thus, we examined whether BMMP affects CA-CA interaction using purified CA. An *in vitro* assembly reaction with purified HIV-1 CA was employed to test if BMMP disrupted CA-CA interactions. *In vitro* assembly reaction of CA has shown it to produce tubular structures representing the mature CA capsid structure (17, 36). We added BMMP to the *in vitro* assembly reaction with 100 μM HIV-1 CA, and resultant CA assembly products were observed by electron microscopy (Fig. 7A). For quantitative analysis, the resultant CA assembly products were recovered by ultracentrifugation and subjected to SDS-PAGE. The levels of the CA assembly products were reduced when BMMP was added at a concentration higher than 30 μM, corresponding to approximately a 1:3 molar ratio to CA (Fig. 7A). These data suggest that BMMP targets HIV-1 CA and leads to the destabilization of the viral capsid core, since our previous findings indicated that BMMP did not block particle release (Fig. 4) but did block the HIV-1 infection postentry (Fig. 5).

To test this possibility in a more relevant assay, we adopted cell-free disassembly assays using purified HIV-1 mature capsid core. To this end, we isolated HIV-1 capsid cores by ultracentrifugation through a Triton X-100 layer, as described pre-

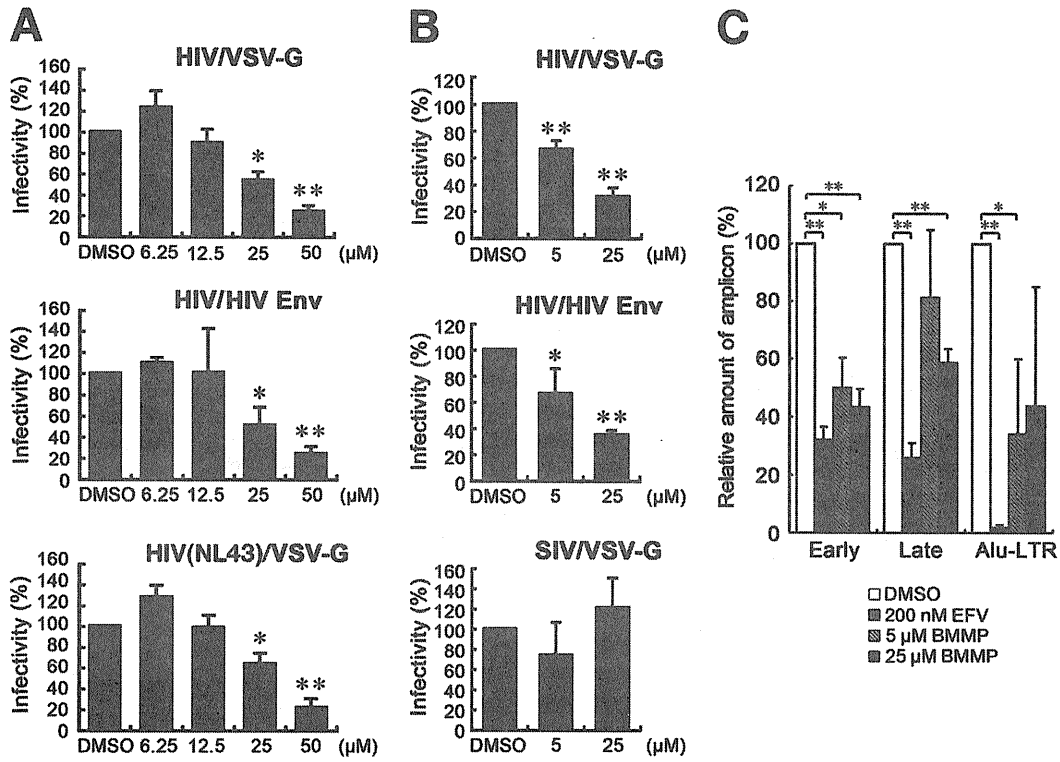

FIG. 5. Inhibition of HIV-1 replication postentry. (A) Single-round infection assays in MT-4 cells. 293FT cells were cotransfected with pHIVgag-pol (derived from HXB2 strain), pLenti-luciferase, pRevpac, and either a plasmid expressing HIV-1 Env (middle) or a plasmid expressing VSV-G (top). HIV-1 (NL43 strain) expressing luciferase was similarly pseudotyped with VSV-G protein (bottom). Following incubation, the culture supernatants were recovered and were subsequently inoculated into MT-4 cells with increasing doses of BMMP. (B) Single-round infection assays in 293FT and 293FT-CD4 cells. HIV-1 vectors containing the luciferase gene were similarly pseudotyped with HIV-1 Env (middle) or VSV-G protein (top). Luciferase-expressing SIVmac was pseudotyped with VSV-G protein by cotransfection (bottom). Viruses produced were subsequently inoculated into 293FT (top and bottom) or 293FT-CD4 (middle) cells with 5 and 25 μM BMMP. Viral infectivity was assessed by luciferase reporter assays. Data were shown as means with standard deviations from 3 to 6 independent experiments in panels A and B. *, $P < 0.05$; **, $P < 0.01$. (C) Quantitative PCR. MT-4 cells were infected with HIV-1 (HXB2 strain) and incubated in the presence of BMMP. DNA was isolated at 4 or 24 h postinfection and subjected to quantitative PCR for HIV cDNA. Reverse transcripts generated at the early and late phases of HIV reverse transcription were amplified from the DNA isolated at 4 and 24 h postinfection, respectively. The integrated viral genome was amplified as *Alu*-LTR transcripts from the DNA isolated at 24 h postinfection. EFV (200 nM) was used as positive controls. Three independent infections were performed, and quantitative PCR was carried out in triplicate with each infection sample. Representative data were shown with the means and standard deviations. *, $P < 0.05$; **, $P < 0.01$.

viously (3). HIV-1 cores are known to disassemble when incubated at 37°C. We examined if BMMP accelerated the rate of core disassembly. The HIV-1 cores were incubated with BMMP at 37°C up to 120 min, and residual intact cores were recovered by centrifugation. When quantified by p24CA antigen capture ELISA, intact cores were found to be reduced in a time-dependent manner in the presence of DMSO (as control), consistent with previous reports (3). A similar level of reduction was observed in the presence of AZT. However, addition of BMMP accelerated a reduction in intact cores in a dose-dependent manner (Fig. 7B). Altogether, our data indicated that BMMP disrupted HIV-1 capsid cores through targeting CA.

DISCUSSION

In this study, we employed a yeast membrane-associated two-hybrid assay to monitor the HIV Gag-Gag interactions and established cell-based screening assays for drugs targeting Gag assembly. We screened a commercially available chemical library and found BMMP, which inhibits HIV-1 replication in PBMC culture. Our single-round infection analysis indicated that BMMP primarily targets HIV-1 CA and inhibits HIV infection postentry but not particle production (Fig. 4 to 6). *In vitro* CA assembly/disassembly assays showed that BMMP facilitated HIV-1 core disassembly (Fig. 7). Collectively, it is conceivable that BMMP may bind to mature capsid structure and facilitate disassembly of the capsid, leading to premature earlier uncoating and failure of postentry events (e.g., reverse transcription and integration). The mechanism of action may be akin to the block of HIV-1 entry by rTRIM5α (30).

Previous studies have reported inhibitors that target HIV-1 Gag assembly and/or Gag processing. 3-*O*-(3′,3′-Dimethylsuccinyl)betulinic acid, known as PA-457 or Bevirimat (molecular weight, 584), binds to the Gag CA-SP1 cleavage site and inhibits proteolytic conversion of Gag precursors to the mature form of p24CA (50% inhibitory concentration [IC_{50}] = 10 nM) (1, 2, 21). Inhibition of Gag processing has also been observed with a distinct chemical class of compound, 1-[2-(4-tert-butylphenyl)-2-(2,3-dihydro-1H-inden-2-ylamino)ethyl]-3-(trifluoro-

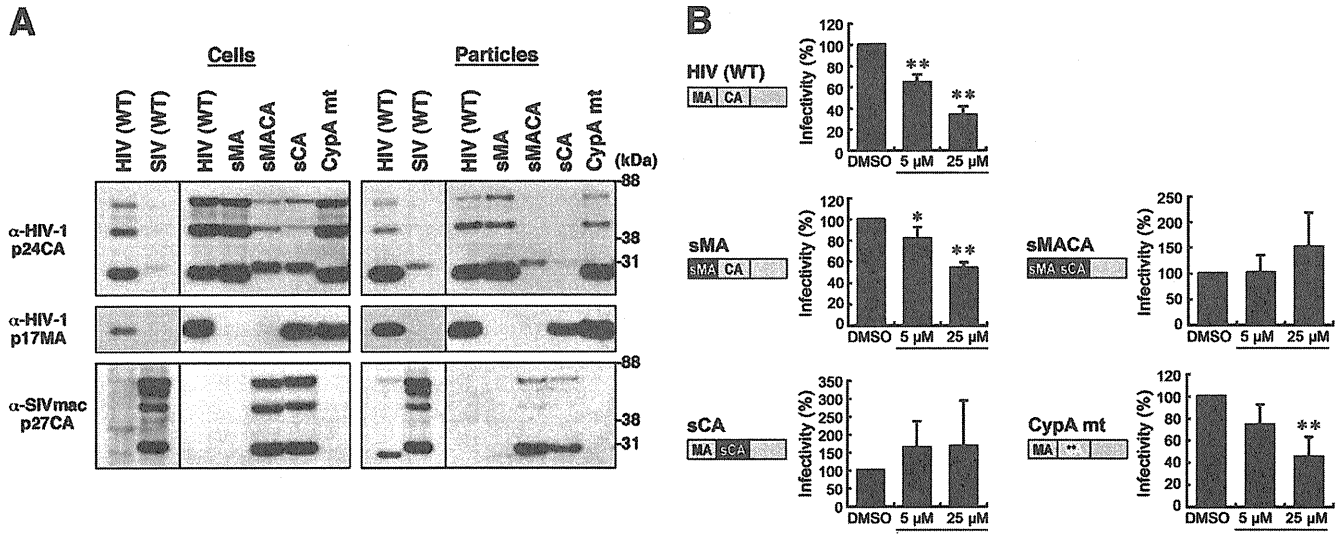

FIG. 6. Mapping of Gag domain responsible for inhibition. (A) Intracellular Gag expression and particle production. 293FT cells were cotransfected with pHIVgag-pol expressing chimeric Gag, pLenti-luciferase, pRevpac, and a plasmid expressing VSV-G, and virus particles produced were purified by ultracentrifugation. Cells and particles were analyzed by Western blotting using anti-HIV-1 p24CA and p17MA and anti-SIVmac p27CA antibodies. (B) Single-round infection assays with the Gag domain chimeras and Gag mutants with amino acid substitutions. The corresponding domain of SIVmac Gag (black) was introduced into HIV-1 Gag background (gray), and the resultant chimera was referred to as "s" plus the name of the corresponding domain of SIVmac. WT, wild type; sMA, HIV containing replacement of MA with SIV MA; sMACA, HIV containing replacement of MACA with SIV MACA; sCA, HIV containing replacement of CA with SIV CA. CypA mt represents HIV with amino acid substitutions G89A and P90A in the CypA-binding loop of CA NTD (denoted by asterisks). Following infection, the cell culture was incubated in the presence of 5 and 25 μM BMMP. Viral infectivity was monitored by luciferase reporter assays. Data were shown as means with standard deviations from 4 to 6 independent experiments. *, $P < 0.05$; **, $P < 0.01$.

methyl)pyridin-2(1H)-one (molecular weight, 454) (7). The hallmark of these inhibitors is incomplete Gag processing and accumulation of processing intermediates (e.g., CA-SP1) in virions, resulting in the loss of viral infectivity. These compounds do not inhibit Gag assembly. Since our BMMP did not show alteration in overall patterns of Gag processing (Fig. 4A), it is unlikely that BMMP shares the inhibition mechanisms with above inhibitors.

Inhibitors of HIV capsid assembly have been extensively screened by several approaches. *In silico* screening from public chemical libraries has identified *N*-(3-chloro-4-methylphenyl)-*N'*-{2-[({5-[(dimethylamino)-methyl]-2-furyl}-methyl)-sulfanyl] ethyl}-urea, termed CAP-1 (32), which binds to HIV-1 CA NTD (K_d [dissociation constant] = 800 μM), resulting in the inhibition of the correct interaction of hexameric units of CA NTD with dimeric units of CA CTD, essential for a high order of CA assembly (20). CAP-1 reduced the infectivity of progeny HIV but did not inhibit viral entry or particle production (32). Phage display biopanning has also been employed and has isolated a 12-mer peptide, termed CAI, which binds to HIV-1 CA CTD (50% inhibitory concentration [IC_{50}] = 3 to 4 μM) and inhibits CA capsid formation *in vitro* (K_d = 15 μM) (5, 29, 33). However, CAI did not inhibit HIV replication in cell culture because of the lack of cell permeability. In a subsequent study, CAI has been converted to a cell-penetrating peptide (termed NYAD-1) by stabilizing the α-helical structure of CAI with a hydrocarbon staple, leading to a marked improvement of K_d (<1 μM) (38). Surprisingly, the study revealed that, besides inhibiting the particle production, NYAD-1 disrupted the mature core formation and inhibited the early stage of HIV-1 in single-round infection assays, suggesting that NYAD-1 may affect the uncoating stage of the HIV life cycle through a mechanism similar to that of BMMP.

The difference between BMMP and CAI/NYAD-1 is that BMMP does not affect HIV-1 particle production or maturation steps. This is possibly because BMMP inhibits CA-CA interactions more efficiently than Gag-Gag interactions. Importantly, BMMP is not a peptide but a low-molecular-weight compound (molecular weight, 273.38), which is chemically and physically stable. It should be possible to chemically modify the BMMP structure to potentiate its biochemical and biological activities. The advantage of BMMP is that, due to its low molecular weight, the derivatives could retain cell membrane permeability unless large chemical groups are attached to the core structure.

A low-molecular-weight Gag inhibitor, PF74, previously screened from a chemical library by a high-throughput single-round infection assay (6), has been characterized by a more recent study, in which PF74 selectively inhibited HIV-1 (27). PF74 destabilized HIV-1 capsids and inhibited the postentry events, similarly to BMMP, but at low-micromolar concentrations. However, BMMP is distinct from PF74 in that the CypA-binding loop is not involved in the viral susceptibility to BMMP (Fig. 6B). Also, BMMP did not reduce the viral infectivity when the virion was exposed to BMMP (data not shown). Therefore, BMMP may have a potential to serve as a lead compound for the development of anti-HIV drugs bearing a novel mechanism of action.

Although BMMP showed anti-HIV activity, it still needs to be improved to lower the IC_{50}. We suggest that comprehensive studies on structural analogues of BMMP would be informative to understand the structure-function relationship of

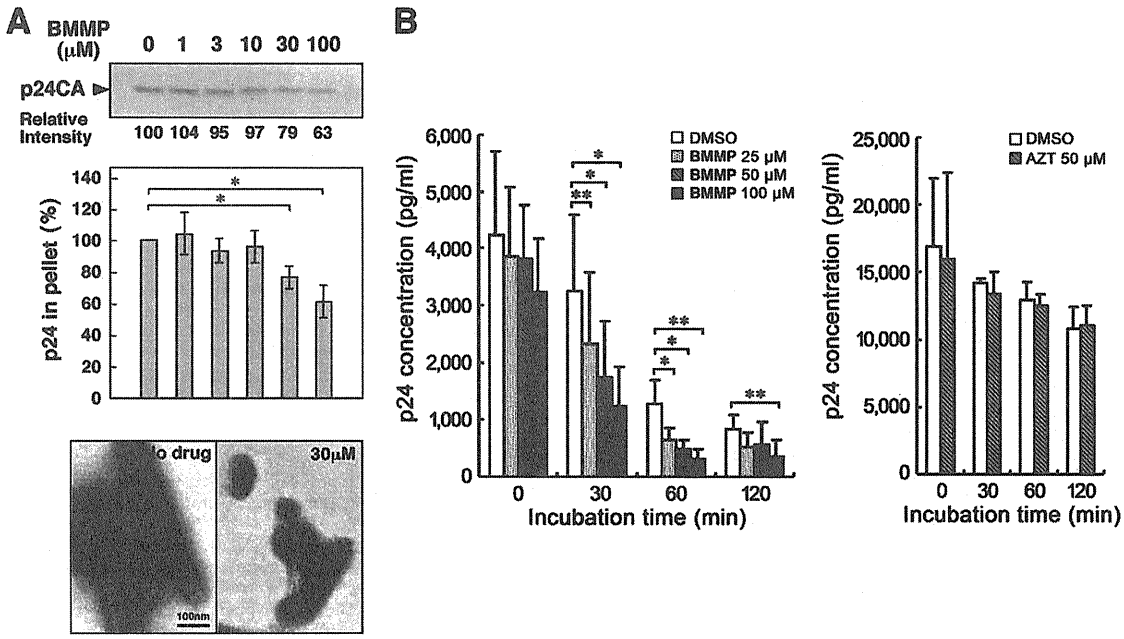

FIG. 7. HIV-1 mature capsid disassembly and *in vitro* assembly assays. (A) *In vitro* assembly reaction with purified HIV-1 CA. Purified HIV-1 CA protein (100 μM) was incubated with various doses of BMMP at 37°C for 60 min in buffer at high salt concentration. All samples included 1% DMSO. Assembly products were recovered by centrifugation and subjected to SDS-PAGE followed by Coomassie brilliant blue staining. The band intensities were semiquantified by ImageJ software. For quantification, the pelleted products were subjected to p24CA antigen capture ELISA. Data were shown as means with standard deviations from 3 independent experiments. *, $P < 0.05$. Assembly products were also negatively stained and examined by electron microscopy. Micrographs were shown at the same magnification. Bar = 100 nm. (B) Cell-free assays for HIV-1 uncoating. HIV-1 mature capsids were isolated through a 1% Triton X-100 layer as described previously (3). The HIV-1 cores were incubated with various doses of BMMP at 37°C up to 120 min. For comparison, the cores were similarly incubated with 50 μM AZT. All samples included 1% DMSO. Residual intact cores were recovered by ultracentrifugation and quantified by p24CA antigen capture ELISA. Data were shown as means with standard deviations from 4 independent experiments. *, $P < 0.05$; **, $P < 0.01$.

BMMP. Also, analysis of BMMP-resistant viruses and X-ray cocrystallography should provide insights into the mechanism of action that direct the way to potentiate the BMMP derivatives.

Recent cryo-electron microscopy and X-ray structure analysis have revealed the intermolecular interfaces between NTD and CTD in the three-dimensional hexameric structures of full-length CA (18, 24). It has been strongly suggested that multiple CA interactions, including NTD-NTD, CTD-CTD, and NTD-CTD, are essential for the constitution of mature HIV capsid. It is possible that some of the interfaces may not be formed in Gag-Gag interactions. CAI, similar to CAP-1, may inhibit CA assembly possibly by disrupting the formation of the NTD-CTD interface (18). Thus, these studies may provide a rationale for developing inhibitors that target the molecular interface of CA that specifically appears during a higher order of oligomerization. We suggest that viral capsid assembly/disassembly is an attractive therapeutic target and that such capsid inhibitors would help understand the regulation of postentry events.

ACKNOWLEDGMENTS

This work was supported by a Human Science grant from the Ministry of Health, Labor, and Welfare of Japan and by a Grant-in-Aid for Scientific Research from the Japan Society for the Promotion of Science.

REFERENCES

1. **Adamson, C. S., et al.** 2006. In vitro resistance to the human immunodeficiency virus type 1 maturation inhibitor PA-457 (Bevirimat). J. Virol. **80:** 10957–10971.
2. **Adamson, C. S., K. Waki, S. D. Ablan, K. Salzwedel, and E. O. Freed.** 2009. Impact of human immunodeficiency virus type 1 resistance to protease inhibitors on evolution of resistance to the maturation inhibitor bevirimat (PA-457). J. Virol. **83:**4884–4894.
3. **Aiken, C.** 2009. Cell-free assays for HIV-1 uncoating. Methods Mol. Biol. **485:**41–53.
4. **Aronheim, A., et al.** 1994. Membrane targeting of the nucleotide exchange factor Sos is sufficient for activating the Ras signaling pathway. Cell **78:**949–961.
5. **Bartonova, V., et al.** 2008. Residues in the HIV-1 capsid assembly inhibitor binding site are essential for maintaining the assembly-competent quaternary structure of the capsid protein. J. Biol. Chem. **283:**32024–32033.
6. **Blair, W. S., et al.** 2005. A novel HIV-1 antiviral high throughput screening approach for the discovery of HIV-1 inhibitors. Antiviral Res. **65:**107–116.
7. **Blair, W. S., et al.** 2009. New small-molecule inhibitor class targeting human immunodeficiency virus type 1 virion maturation. Antimicrob. Agents Chemother. **53:**5080–5087.
8. **Botstein, D.** 1997. Yeast as a model organism. Science **277:**1259–1260.
9. **Braaten, D., E. K. Franke, and J. Luban.** 1996. Cyclophilin A is required for an early step in the life cycle of human immunodeficiency virus type 1 before the initiation of reverse transcription. J. Virol. **70:**3551–3560.
10. **Broder, S.** 2010. The development of antiretroviral therapy and its impact on the HIV-1/AIDS pandemic. Antiviral Res. **85:**1–18.
11. **Bukovsky, A. A., A. Weimann, M. A. Accola, and H. G. Gottlinger.** 1997. Transfer of the HIV-1 cyclophilin-binding site to simian immunodeficiency virus from *Macaca mulatta* can confer both cyclosporin sensitivity and cyclosporin dependence. Proc. Natl. Acad. Sci. U. S. A. **94:**10943–10948.
12. **Butler, S. L., M. S. T. Hansen, and F. D. Bushman.** 2001. A quantitative assay for HIV DNA integration *in vivo*. Nat. Med. **7:**631–634.
13. **Craven, R. C., and L. J. Parent.** 1996. Dynamic interactions of the Gag polyprotein. Curr. Top. Microbiol. Immunol. **214:**65–94.
14. **Forshey, B. M., U. von Schwedler, W. I. Sundquist, and C. Aiken.** 2002.

Formation of a human immunodeficiency virus type 1 core of optimal stability is crucial for viral replication. J. Virol. **76:**5667–5677.
15. **Franke, E. K., H. E. Yuan, and J. Luban.** 1994. Specific incorporation of cyclophilin A into HIV-1 virions. Nature **372:**359–362.
16. **Gamble, T. R., et al.** 1996. Crystal structure of human cyclophilin A bound to the amino-terminal domain of HIV-1 capsid. Cell **87:**1285–1294.
17. **Ganser, B. K., S. Li, V. Y. Klishko, J. T. Finch, and W. I. Sundquist.** 1999. Assembly and analysis of conical models for the HIV-1 core. Science **283:** 80–83.
18. **Ganser-Pornillos, B. K., A. Cheng, and M. Yeager.** 2007. Structure of full-length HIV-1 CA: a model for the mature capsid lattice. Cell **131:**70–79.
19. **Graf Einsiedel, H., et al.** 2002. Deletion analysis of $p16^{INKa}$ and $p15^{INKb}$ in relapsed childhood acute lymphoblastic leukemia. Blood **99:**4629–4631.
20. **Kelly, B. N., et al.** 2007. Structure of the antiviral assembly inhibitor CAP-1 complex with the HIV-1 CA protein. J. Mol. Biol. **373:**355–366.
21. **Li, F., et al.** 2003. PA-457: a potent HIV inhibitor that disrupts core condensation by targeting a late step in Gag processing. Proc. Natl. Acad. Sci. U. S. A. **100:**13555–13560.
22. **Morikawa, Y.** 2003. HIV capsid assembly. Curr. HIV Res. **1:**1–14.
23. **Pauwels, R., et al.** 1990. Potent and selective inhibition of HIV-1 replication in vitro by a novel series of TIBO derivatives. Nature **343:**470–474.
24. **Pornillos, O., et al.** 2009. X-ray structures of the hexameric building block of the HIV capsid. Cell **137:**1282–1292.
25. **Roberts, N. A., et al.** 1990. Rational design of peptide-based HIV proteinase inhibitors. Science **248:**358–361.
26. **Sakuragi, S., T. Goto, K. Sano, and Y. Morikawa.** 2002. HIV type 1 Gag virus-like particle budding from spheroplasts of *Saccharomyces cerevisiae*. Proc. Natl. Acad. Sci. U. S. A. **99:**7956–7961.
27. **Shi, J., J. Zhou, V. B. Shah, C. Aiken, and K. Whitby.** 2011. Small molecule inhibition of human immunodeficiency virus type 1 infection by virus capsid destabilization. J. Virol. **85:**542–549.
28. **Shimizu, S., et al.** 2007. Inhibiting lentiviral replication by HEXIM1, a cellular negative regulator of the CDK9/cyclin T complex. AIDS **21:**575–582.
29. **Sticht, J., et al.** 2005. A peptide inhibitor of HIV-1 assembly *in vitro*. Nat. Struct. Mol. Biol. **12:**671–677.
30. **Stremlau, M., et al.** 2006. Specific recognition and accelerated uncoating of retroviral capsids by the TRIM5alpha restriction factor. Proc. Natl. Acad. Sci. U. S. A. **103:**5514–5519.
31. **Suzuki, S., et al.** 2010. Peptide HIV-1 integrase inhibitors from HIV-1 gene products. J. Med. Chem. **53:**5356–5360.
32. **Tang, C., et al.** 2003. Antiviral inhibition of the HIV-1 capsid protein. J. Mol. Biol. **327:**1013–1020.
33. **Ternois, F., J. Sticht, S. Duquerroy, H. G. Krausslich, and F. A. Rey.** 2005. The HIV-1 capsid protein C-terminal domain in complex with a virus assembly inhibitor. Nat. Struct. Mol. Biol. **12:**678–682.
34. **Towers, G. J., et al.** 2003. Cyclophilin A modulates the sensitivity of HIV-1 to host restriction factors. Nat. Med. **9:**1138–1143.
35. **Urano, E., et al.** 2008. Substitution of the myristoylation signal of human immunodeficiency virus type 1 Pr55Gag with the phospholipase C-delta1 pleckstrin homology domain results in infectious pseudovirion production. J. Gen. Virol. **89:**3144–3149.
36. **von Schwedler, U. K., et al.** 1998. Proteolytic refolding of the HIV-1 capsid protein amino-terminus facilitates viral core assembly. EMBO J. **17:**1555–1568.
37. **Westby, M., G. R. Nakayama, S. L. Butler, and W. S. Blair.** 2005. Cell-based and biochemical screening approaches for the discovery of novel HIV-1 inhibitors. Antiviral Res. **67:**121–140.
38. **Zhang, H., et al.** 2008. A cell-penetrating helical peptide as a potential HIV-1 inhibitor. J. Mol. Biol. **378:**565–580.

frontiers in
MICROBIOLOGY

ORIGINAL RESEARCH ARTICLE
published: 10 January 2012
doi: 10.3389/fmicb.2011.00280

Fluorescent reporter signals, EGFP, and DsRed, encoded in HIV-1 facilitate the detection of productively infected cells and cell-associated viral replication levels

Kazutaka Terahara[1], Takuya Yamamoto[2], Yu-ya Mitsuki[1,3], Kentaro Shibusawa[1,3], Masayuki Ishige[1,4], Fuminori Mizukoshi[5], Kazuo Kobayashi[1] and Yasuko Tsunetsugu-Yokota[1]*

[1] Department of Immunology, National Institute of Infectious Diseases, Tokyo, Japan
[2] The Immunology Laboratory, Vaccine Research Center, National Institute of Allergy and Infectious Diseases, National Institutes of Health, Bethesda, MD, USA
[3] Research Resident, Japan Foundation for AIDS Prevention, Tokyo, Japan
[4] Division of Hematopoiesis, Center for AIDS Research, Kumamoto University, Kumamoto, Japan
[5] Department of Microbiology, The Tochigi Prefectural Institute of Public Health and Environmental Science, Tochigi, Japan

Edited by:
Hirofumi Akari, Kyoto University, Japan

Reviewed by:
Mikako Fujita, Kumamoto University, Japan
Jun-Ichi Sakuragi, Osaka University, Japan

***Correspondence:**
Yasuko Tsunetsugu-Yokota, Department of Immunology, National Institute of Infectious Diseases, 1-23-1 Toyama, Shinjuku-ku, Tokyo 162-8640, Japan.
e-mail: yyokota@nih.go.jp

Flow cytometric analysis is a reliable and convenient method for investigating molecules at the single cell level. Previously, recombinant human immunodeficiency virus type 1 (HIV-1) strains were constructed that express a fluorescent reporter, either enhanced green fluorescent protein, or DsRed, which allow the monitoring of HIV-1-infected cells by flow cytometry. The present study further investigated the potential of these recombinant viruses in terms of whether the HIV-1 fluorescent reporters would be helpful in evaluating viral replication based on fluorescence intensity. When primary CD4$^+$ T cells were infected with recombinant viruses, the fluorescent reporter intensity measured by flow cytometry was associated with the level of CD4 downmodulation and Gag p24 expression in infected cells. Interestingly, some HIV-1-infected cells, in which CD4 was only moderately downmodulated, were reporter-positive but Gag p24-negative. Furthermore, when the activation status of primary CD4$^+$ T cells was modulated by T cell receptor-mediated stimulation, we confirmed the preferential viral production upon strong stimulation and showed that the intensity of the fluorescent reporter within a proportion of HIV-1-infected cells was correlated with the viral replication level. These findings indicate that a fluorescent reporter encoded within HIV-1 is useful for the sensitive detection of productively infected cells at different stages of infection and for evaluating cell-associated viral replication at the single cell level.

Keywords: HIV-1, flow cytometry, EGFP, DsRed, Gag, productive infection

INTRODUCTION

Human immunodeficiency virus type 1 (HIV-1) interacts with its primary receptor, CD4, and a co-receptor, usually CCR5 or CXCR4, to infect T cells, macrophages, and dendritic cells (Mcclure et al., 1987; Berger et al., 1999; Tsunetsugu-Yokota, 2008). Single cell analysis of HIV-1-infected cells is an essential approach to investigate the differential dynamics of HIV-1 infection and the cellular consequences for each of the HIV-1-targeted cell populations. To monitor HIV-1 infection, a recombinant HIV-1 encoding a reporter luciferase (Luc) gene, or indicator cells transduced with enzymatic reporters such as Luc, β-galactosidase, alkaline phosphatase, and chloramphenicol acetyl transferase, incorporated downstream of the HIV-1 long terminal repeats (LTR) have been widely used (Kar-Roy et al., 2000). However, these reporters require additional substrates or co-factors, and lysis or fixation of cells is required to show reporter activity, which makes the experimental process more complex. In addition, it is difficult to distinguish infected cells from uninfected cells using these reporter assays.

An alternative molecule, green fluorescent protein (GFP) and/or its derivatives, is a powerful reporter that does not require any substrates and co-factors to generate a reporter signal (Chalfie, 1995; Cubitt et al., 1995; Heim et al., 1995). Page et al. (1997) first used a GFP derivative, called enhanced green fluorescent protein (EGFP), as a fluorescent reporter molecule for HIV-1 and showed that infected cells were detectable and, more importantly, distinguishable from uninfected cells using flow cytometry. Furthermore, a red fluorescent protein, DsRed, has been used as an HIV-1 fluorescent reporter (Weber et al., 2006). The main benefit of such recombinant HIV-1 molecules is that the targeted cells do not require any modulation (e.g., transfection) of exogenous reporter genes and, therefore, they allow the characterization of intact HIV-1-infected cells. In most cases of previous recombinant HIV-1 strains, the *nef* gene was replaced with a reporter gene. Therefore, we previously constructed *nef*-intact, replication-competent, recombinant HIV-1 strains encoding either EGFP or DsRed, and showed that CXCR4-tropic X4 and CCR5-tropic R5 viruses replicate differently in CD4$^+$ T cells simultaneously infected with X4 HIV-1 encoding EGFP and R5 HIV-1 encoding

DsRed (Yamamoto et al., 2009). Such recombinant HIV-1 strains encoding a fluorescent reporter gene will be even more valuable because of recent advances in multicolor flow cytometry, which permit more detailed characterization of HIV-1-infected cells.

Flow cytometry is a reliable and convenient method for analysis at the single cell level. Because the transcriptional activity of HIV-1 can be quantitatively monitored in indicator cells according to the fluorescence intensity of an EGFP reporter driven by the HIV-1 LTR (Dorsky et al., 1996; Gervaix et al., 1997; Kar-Roy et al., 2000), we investigated whether the HIV-1-expressing fluorescent reporters EGFP and DsRed would allow the quantitative evaluation of viral replication using a flow cytometer. The results show that a fluorescent reporter signal generated by recombinant HIV-1 strains enables the detection of infected cells at various stages of the viral life cycle.

MATERIALS AND METHODS

CELL PREPARATION

Human peripheral blood samples were collected from healthy donors after written informed consent. Sample collection was approved by the Institutional Ethical Committee of the National Institute of Infectious Diseases (NIID; Tokyo, Japan). Peripheral blood mononuclear cells (PBMCs) were separated on a Ficoll–Hypaque density gradient (Lymphosepal; IBL, Gunma, Japan) and $CD4^+$ T cells were negatively selected from the PBMCs using an EasySep Human $CD4^+$ T cell Enrichment Kit (StemCell Technologies, Vancouver, BC, Canada).

CEM cells stably expressing human CCR5 (CEM–CCR5) were established by transducing CEM cells with the human *ccr5* gene using a conventional mouse retrovirus system. CEM–CCR5 cells were maintained in complete RPMI medium (10% heat-inactivated fetal bovine serum, 100 μg/ml penicillin, 100 μg/ml streptomycin, and 2 mM L-glutamine) supplemented with 1 μg/ml puromycin at 37°C.

PREPARATION OF HIV-1 VIRUS STOCKS

We previously constructed pNL432-based proviral clones encoding EGFP (pNL-E) or DsRed (pNL-D) for X4-tropic HIV-$1_{NL\text{-}E}$ or HIV-$1_{NL\text{-}D}$, respectively, and pNLAD8-based proviral clones encoding EGFP (pNLAD8-E) or DsRed (pNLAD8-D) for R5-tropic HIV-$1_{NLAD8\text{-}E}$ or HIV-$1_{NLAD8\text{-}D}$, respectively (Yamamoto et al., 2009; **Figure 1**). To prepare the HIV-1 viral stocks, the human embryonic kidney cell line 293T was transfected with pNL-E, pNL-D, pNLAD8-E, or pNLAD8-D using the calcium phosphate precipitation method and then incubated for 48 h. Culture supernatants were filtered and frozen at −80°C. The amount of virus in each culture supernatant was measured using an in-house HIV-1 Gag p24 enzyme-linked immunosorbent assay (ELISA; Tsunetsugu-Yokota et al., 1995).

STIMULATION OF T CELL RECEPTORS

T cell receptors (TCR) were stimulated as described previously (Yamamoto et al., 2009) with some modifications. In brief, primary $CD4^+$ T cells were suspended in complete RPMI medium supplemented with 5% human plasma and stimulated with 5 μg/ml of immobilized anti-human CD3 monoclonal antibody (mAb; eBioscience, San Diego, CA) and 1 μg/ml of soluble anti-human CD28 mAb (eBioscience) in U-bottom, 96-well plates at 37°C for 4 (weak stimulation) or 24 h (strong stimulation).

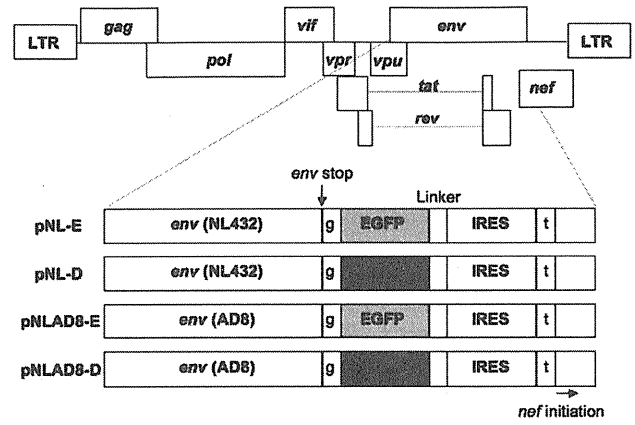

FIGURE 1 | Structure of the proviral DNA. The pNL432-based proviral clones encoded EGFP (pNL-E) or DsRed (pNL-D) for X4-tropic HIV-$1_{NL\text{-}E}$ or HIV-$1_{NL\text{-}D}$, respectively, and the pNLAD8-based proviral clones encoded EGFP (pNLAD8-E) or DsRed (pNLAD8-D) for R5-tropic HIV-$1_{NLAD8\text{-}E}$ or HIV-$1_{NLAD8\text{-}D}$, respectively. EGFP or DsRed was not expressed as a fusion protein with Env due to the insertion of a single base after the Env stop codon. Nef was also independently expressed under the control of IRES. t (Thymine) and g (guanine) are additional DNA sequences.

HIV-1 INFECTION AND CELL CULTURE

Primary $CD4^+$ T cells (either unstimulated or pre-TCR-stimulated) or CEM–CCR5 cells were infected with 200 ng of p24-measured amounts of HIV-$1_{NL\text{-}E}$, HIV-$1_{NL\text{-}D}$, HIV-$1_{NLAD8\text{-}E}$, or HIV-$1_{NLAD8\text{-}D}$ per 1×10^6 cells by spinoculation at $1200 \times g$ for 2 h at 25 (conventional conditions) or 4°C (for CEM–CCR5 cells), as described previously (O'doherty et al., 2000; Dai et al., 2009). After spinoculation, cells were washed three times with PBS. Primary $CD4^+$ T cells were then suspended in complete RPMI medium supplemented with 5% human plasma. The cell suspensions derived from unstimulated or pre-TCR-stimulated $CD4^+$ T cells were settled onto U-bottom, 96-well plates with or without TCR-stimulation, respectively, at 37°C for 24 h. After the 24 h culture, cells were washed three times with PBS, suspended in complete RPMI medium supplemented with 5% human plasma and 50 U/ml recombinant interleukin-2, and cultured in U-bottom, 96-well plates at 37°C for up to 4 days.

FLOW CYTOMETRY

Cells were stained with fluorescence-conjugated mAbs as described previously (Yamamoto et al., 2009). The following mAbs were used for flow cytometry in various combinations: Pacific Blue-conjugated anti-human CD3 mAb (BioLegend, San Diego, CA, USA), phycoerythrin Cy7-conjugated anti-human CD4 mAb (BioLegend), and Alexa Fluor 700-conjugated anti-human CD8a mAb (BioLegend); and Nu24 mAb specific for HIV-1 Gag p24 (kindly provided by Dr. T. Sata, NIID, Tokyo, Japan) and conjugated to Alexa Fluor 647 using an Alexa Fluor 647 Protein Labeling Kit (Molecular Probes, Eugene, OR, USA). Dead cells were stained with propidium iodide or a LIVE/DEAD Fixable Dead Cell Stain

Kit (L34957; Invitrogen, Carlsbad, CA, USA). Intracellular staining (ICS) by Nu24 mAb was performed using a FIX and PERM Fixation and Permeabilization Kit (Invitrogen). Data collection was performed using a FACSCanto II (BD Bioscience, San Diego, CA, USA) and the data were analyzed using FACSDiva software (BD Bioscience) and FlowJo software (Tree Star, San Carlos, CA, USA).

QUANTIFICATION OF REPLICATED HIV-1 IN CELL CULTURE SUPERNATANTS

Human immunodeficiency virus type 1 replication was quantified in cell culture supernatants by ELISA and real-time RT-PCR. Gag p24 was measured using a RETRO-TEK HIV-1 p24 Antigen ELISA (ZeptoMetrix Corporation, Buffalo, NY, USA). For real-time RT-PCR, viral RNA was extracted using a QIAamp Viral RNA Mini Kit (Qiagen, Valencia, CA, USA) and subjected to real-time RT-PCR using a SuperScript III Platinum One-Step Quantitative RT-PCR System (Invitrogen), a set of HIV-1 *gag*-targeted primers, and a TaqMan probe as previously described (Saito et al., 2010). PCR was performed in an Mx3000P (Stratagene, La Jolla, CA, USA).

RESULTS

CD4 DOWNMODULATION IS ASSOCIATED WITH HIV-1 FLUORESCENT REPORTER INTENSITY

The cell surface CD4 molecule is downmodulated in HIV-1-infected cells in response to the HIV-1 components Env, Nef, and Vpu (Malim and Emerman, 2008). Therefore, to investigate the correlation between the level of CD4 downmodulation and the HIV-1 fluorescent reporter intensity, primary $CD4^+$ T cells infected with HIV-$1_{NL\text{-}E}$, HIV-$1_{NL\text{-}D}$, HIV-$1_{NLAD8\text{-}E}$, or HIV-$1_{NLAD8\text{-}D}$ followed by TCR-stimulation for 1 day and cultivation for a further 4 days were analyzed by flow cytometry. As shown in **Figure 2** (left panels), HIV-1-infected cells expressing a fluorescent reporter signal, EGFP, or DsRed, were detected, although the numbers varied between individual donors ($n = 3$–4): about 10–30% for X4-tropic HIV-$1_{NL\text{-}E}$-infected and HIV-$1_{NL\text{-}D}$-infected cells and 1–10% for R5-tropic HIV-$1_{NLAD8\text{-}E}$-infected and HIV-$1_{NLAD8\text{-}D}$-infected cells. However, the number of HIV-1^+ cells was comparable between HIV-$1_{NL\text{-}E}$ and HIV-$1_{NL\text{-}D}$ (X4-tropic), and between HIV-$1_{NLAD8\text{-}E}$ and HIV-$1_{NLAD8\text{-}D}$ (R5-tropic) within each donor, showing that the fluorescent reporter genes encoded within the HIV-1 proviral genome did not affect HIV-1 infectivity as described previously (Yamamoto et al., 2009). When we categorized $CD3^+CD8^-$ T cells into three fractions (HIV-1-negative, -dull, and -high) based on the fluorescence intensity of EGFP and DsRed, we found that CD4 was strongly downmodulated in the HIV-1 high fraction in all the HIV-1 strains (**Figure 2**, right panels). Interestingly, CD4 was also downmodulated in the HIV-1 dull fraction, but the level was modest compared with that in the HIV-1 high fraction (**Figure 2**, right panels). These results indicate that the level of CD4 downmodulation is associated with HIV-1 fluorescent reporter intensity.

FIXATION/PERMEABILIZATION WEAKENS THE HIV-1 FLUORESCENT REPORTER SIGNAL

To investigate the correlation between HIV-1 fluorescent reporter intensity and viral replication levels, we attempted to perform ICS for Gag p24 in HIV-1-infected cells prepared as described above. When we observed X4-tropic HIV-$1_{NL\text{-}E}$-infected and HIV-$1_{NL\text{-}D}$-infected cells from three donors by flow cytometry, we noticed that fixation/permeabilization, an essential step for ICS, weakened the fluorescent reporter signal for both EGFP and DsRed. **Figure 3** shows the flow cytometry profiles obtained for EGFP and DsRed at identical photomultiplier tube (PMT) voltages between intact (untreated) cells and fixed/permeabilized cells to visualize the differences in fluorescent reporter intensity. $DsRed^+$ cells were not properly separated from $DsRed^-$ cells within the population treated by fixation/permeabilization; the frequency of $DsRed^+$ cells was, therefore, markedly decreased. No adjustment of the flow cytometer settings, including PMT voltage and compensation, improved the blunted fluorescent reporter signal generated after fixation/permeabilization. Nevertheless, the number of $EGFP^+$ cells within the intact cell and fixed/permeabilized cell populations was comparable. Similar results were obtained for R5-tropic HIV-$1_{NLAD8\text{-}E}$ and HIV-$1_{NLAD8\text{-}D}$ (data not shown). Taken together, these results indicate that it is preferable to use an EGFP reporter when the fixation/permeabilization of cells is required.

HIV-1 FLUORESCENT REPORTER SIGNALS RELIABLY DETECT PRODUCTIVELY INFECTED CELLS SHOWING DIFFERENT VIRAL REPLICATION LEVELS

Following the results shown in **Figure 3**, we next assessed viral replication levels in the HIV-$1_{NL\text{-}E}$ infection group (5 days culture) from six donors using Gag p24 ICS (**Figure 4**). A representative flow cytometric analysis showed that not all $EGFP^+$ cells were Gag^+ and *vice versa*. When CD4 expression levels were compared in each of the four cell fractions based on the expression patterns of EGFP and Gag p24 ($EGFP^+Gag^+$, $EGFP^+Gag^-$, $EGFP^-Gag^+$, and $EGFP^-Gag^-$), the strongest downmodulation of CD4 was observed in $EGFP^+Gag^+$ cells (red fraction). CD4 downmodulation was moderate in $EGFP^+Gag^-$ cells (green fraction). However, CD4 was not downmodulated at all in $EGFP^-Gag^+$ cells (blue fraction) and the expression level of CD4 was the same as that in $EGFP^-Gag^-$ cells (black fraction). We further divided the $EGFP^+Gag^+$ cells (red fraction) into Gag^{hi} (brown fraction) and Gag^{lo} cells (pink fraction) and compared the expression levels of EGFP and CD4 with those of Gag p24. Gag^{hi} cells (brown fraction) showed the strongest expression of EGFP and the strongest downmodulation of CD4. Gag^{lo} cells (pink fraction) showed an intermediate level of EGFP expression [between that of Gag^{hi} cells (brown fraction) and that of $EGFP^+Gag^-$ cells (green fraction)] and CD4 expression [between that of Gag^{hi} cells (brown fraction) and $EGFP^-Gag^-$ cells (black fraction)]. These results indicate that the expression level of EGFP correlates with that of Gag p24 in HIV-1-infected cells in which CD4 is downmodulated.

HIV-1-BOUND OR -INTERNALIZED CELLS ARE ALSO DETECTED BY Gag p24 ICS

Because CD4 downmodulation was not observed in $EGFP^-Gag^+$ cells (**Figure 4**; blue fraction), it is possible that these cells may still be bound by or have internalized HIV-1 but have not produced virions. Therefore, we next investigated the kinetics of $EGFP^-Gag^+$ cells during 5 days post-infection. Primary $CD4^+$